Medizinische Fakultät
der
Universität Duisburg-Essen

Aus der Klinik für Dermatologie
Arbeitsgruppe „Molekulare Tumorimmunologie“

Characterization of HLA class II negative and HLA class II positive subpopulations from melanoma metastases

I n a u g u r a l d i s s e r t a t i o n
zur
Erlangung des Doktorgrades der Medizin
durch die Medizinische Fakultät
der Universität Duisburg-Essen

Vorgelegt von
Philip Niklas Meerman
aus Stockholm
2021

DOI: 10.17185/duepublico/74841
URN: urn:nbn:de:hbz:464-20211019-150919-0

Dekan:	Herr Univ.-Prof. Dr. med. J. Buer
1. Gutachter:	Frau Prof. Dr. rer. nat. A. M. Paschen
2. Gutachter:	Frau Univ.-Prof. Dr. rer. nat. W. Hansen

Tag der mündlichen Prüfung: 7. September 2021

TABLE OF CONTENTS

Page

1 INTRODUCTION

1.1 Melanoma

The number of patients diagnosed with melanoma is increasing worldwide. In 2012 the incidence was 10.2 per 100,000 person-years in the EU and 13.8 per 100.000 person-years in North America, predominantly increasing among the fair skinned population (Schadendorf et al., 2018). The United States are averaging an increase of 1.4% in melanoma cases annually. Unlike other solid tumors, melanoma mostly affects young and middle-aged individuals (median age at diagnosis, 57 years). In terms of the incidence rate, women are more frequent in younger aged groups, while the men are predominantly affected from the age of 55 onwards. When diagnosed and treated at an early stage (I-II) the 5 year relative survival in the USA exceeds 90%. However due to the often quick dissemination of tumor cells into organs and lymph nodes even at very early stages of the disease the median survival of patient's diagnosed with malignant melanoma has long been unfavorable. The introduction and combination of new therapeutic options over the past few years has improved the progression free survival (PFS) in a subset of stage IV melanoma patients from formerly 7-9 months up to 11-14,9 months, with 40% of patients reaching an overall survival of 3-5 years even. Combining new treatment therapies and identifying resistance mechanisms to treatment remains the main task of therapy improvement in advanced melanoma patients (Schadendorf et al., 2018).

1.2 Development of Melanoma

Melanoma is a form of cancer originating from melanocytes, pigment bearing cells which are primarily situated in the basal layers of our skin, eyes and mucosa. When functioning physiologically, melanocytes produce the pigment melanin which protects the skin from UV mediated DNA damages. Continuous exposure to UV light or intermittent exposure to high doses of UV light can induce irreversible damage to the DNA of melanocytes leading to malignant transformation of the cells. Further predisposing risk factors include genetic factors such as a fair skin color, propensity to burn during tanning, a history of melanoma in the family and the presence of

dysplastic naevi as well as environmental factors like geographic latitude and cumulative UV exposure (Psaty et al., 2010).

There are several steps necessary for the oncogenic transformation of a melanocyte into melanoma. However, some stages vary or can be skipped depending on the type of melanoma. Recent observations concerning histology, pathology and genetics show that the different types of melanoma depend on cell origin, amount of UV-induced damage (CSD = Chronic sun damage), nature of the precursor lesion as well as the type of somatic mutations (Shain & Bastian, 2016).

Following an initiating mutation (predominantly in the $BRAF^{V600E}$ gene) a melanocyte may proliferate into a naevus, in most cases in form of a common acquired naevus in the early years of adolescence. The term common naevus has to be distinguished from the dysplastic naevus as the latter is usually the result of an acquired mutation that serves as a proliferation trigger in melanocytes already harboring pre-existing pathogenic mutations. Their genetic mutations have been shown to differ from those found in common naevi. Despite its initiating mutation a common naevus is generally regarded as benign, but further mutational events (e.g. Telomerase reverse transcriptase (*TERT)* promoter mutations or cyclin dependent kinase inhibitor 2A (*CDKN2A)* loss) can lead to melanoma development. Melanomas deriving from these common naevi usually show a pagetoid growth pattern (“upward spreading”) where the enlarged melanocytes they originate from are scattered through all layers of the epidermis either individually or in nests. Non-CSD melanomas which are commonly found on areas of the body not exposed to direct sun light are associated to these benign precursor naevi.

In contrast, melanomas deriving from CSD are generally not linked to preexisting naevi but rather develop from melanocytes that have been exposed to a high cumulation of UV-induced damage. These melanomas often originate from individual melanocytes situated in the basilar epidermis of the skin. These mutated melanocytes show a high burden of genetic alterations acquired over many years and explain their often late onset in older individuals. They show a typical lentiginous growth pattern where they can spread over several square centimeters of skin as a melanoma *in situ* (Lentigo maligna) before they eventually break through the basilar layer of the skin becoming invasive and gaining access to blood- and lymph vessels (Lentigo maligna melanoma) if not treated appropriately (Shain & Bastian, 2016).

1.3 Molecular mechanisms of melanoma development

There are diverse molecular mechanisms that play a role in the development of melanoma cells. The most common (at least 70%) mutations induce a constitutive activation of the mitogen-activated protein kinase (MAPK) signaling pathway leading to oncogenic cell proliferation and escape from apoptosis. Approximately 50% of melanoma patients express a mutant *BRAF* ($BRAF^{V600E}$) protein, with 90% involving the substitution of Valine to Glutamic acid at position 600 within the serine–threonine kinase, leading to activation of downstream kinases MEK and ERK. Around 15-20% of melanoma tumors harbor an activating mutation in the NRAS gene, encoding the G-protein NRAS, with the protein then no longer depending on ligands to activate the MAPK pathway. *NRAS* mutant melanomas ($NRAS^{Q61K}$, $NRAS^{Q61R}$) are commonly found in older adults with intermittent/chronic sun damage to their skin, while *BRAF* mutant tumors usually affect younger adults without chronic sun damage. Both mutations are generally found to be mutually exclusive (Homet & Ribas, 2014).

Further significant mutations in more advanced melanoma are those affecting the phosphoinositide 3-kinase (PI3K)/ Protein Kinase B (AKT) pathway. Inactivating mutations in the phosphatase and tensin homologue (PTEN), a tumor suppressor gene located on chromosome 10, are present in melanomas showing advanced progression. PTEN negatively regulates the PI3K/AKT pathway by dephosphorylation of phosphatidylinositol-3,4,5-trisphosphate (PIP3) to phosphatidylinositol-3,4,5-diphosphate (PIP2), therefore its inactivation leads to a vast accumulation of PIP3 which in return increases the phosphorylation and activity levels of AKT. AKT is found in the cytosol in an inactive conformation. Upon PI3K activation it translocates to the plasma membrane and undergoes a conformational change via phosphorylation by interaction with PIP3. Once AKT is phosphorylated at two sites it becomes a downstream effector of the PI3K pathway, inhibiting or activating a variety of targets (especially mechanistic Target of Rapamycin (mTOR)) regulating important cellular behaviors such as apoptosis, DNA repair, cell cycle, glucose metabolism, cell growth, motility, invasion, and angiogenesis (Dantonio et al., 2018; Ming et al., 2009; Wu et al., 2003). The result is decreased apoptosis and/or increased mitogen signaling in melanoma cells (Stahl et al., 2003). Studies have reported PTEN mutations in melanoma cell lines, primary melanomas and

metastatic melanoma biopsies, with a frequency of 27.6%, 7.3%, and 15.2%, respectively (Aguissa-Touré et al., 2012).

AKT, also known as protein kinase B, has three isoforms AKT1 (PKBα), AKT2 (PKBβ), and AKT3 (PKBγ). Among the different isoforms, AKT3 has shown to play a key role in melanoma development with high activity levels reported in sporadic melanomas (Madhunapantula & Robertson, 2011). Recent studies find that the AKT pathway is activated in up to 70% of sporadic melanomas promoting cell survival by deregulation of apoptotic signaling (Kuzu et al., 2018) often as a consequence of activating *NRAS* mutations (mutated NRAS signals via the PI3K/AKT pathway), PTEN mutations/loss and activating mutations in specific PI3K subunits, leading to a further often parallel functioning mechanism of cell proliferation working besides or synergistically to that of the MAPK pathway. Additionally, AKT3 has been shown to promote melanoma development from melanocytes and naevi harboring a mutant $BRAF^{V600E}$ mutation. The mutant protein's high level of signaling activity can lead to cell cycle arrest or senescence but secondary mutations in the PI3K/AKT pathway decrease the RAS-ERK signaling to a degree that promotes further transformation (Cheung et al., 2008).

Microphthalmia-associated transcription factor (MITF) acts as a master regulator of melanocyte differentiation, development, function and survival by modulating various differentiation and cell-cycle progression genes (Levy et al., 2006). Low levels of MITF have been linked to a loss/decrease of differentiation and higher invasiveness in patients whereas increased MITF expression leads to decreased invasiveness (Carreira et al., 2006).

In terms of familial predisposition many melanoma cases are linked to mutation, deletion or transcriptional silencing of the afore mentioned *CDKN2A* gene which encodes for the tumor suppressor and cell cycle regulator $p16^{INK4a}$. *CDKN2A* silencing is regarded as an early event in invasive melanoma and is usually not found in precursor lesions (Shain & Bastian, 2016). $p16^{INK4a}$ is a cyclin-dependent kinase inhibitor that plays an important role in the cell cycle by negatively regulating CDK4 which is responsible for the phosphorylation of Retinoblastoma Protein (RB). Phosphorylated RB leads to cell cycle progression, therefore loss of $p16^{INK4a}$ helps affected cells overcome cell cycle arrest (Serrano, 1997; Hodis et al., 2012).

1.4 Therapy options for melanoma

If diagnosed at an early stage (primary melanoma), the primary treatment is local surgical excision with different safety margins depending on the thickness of the melanoma. Lymph node biopsies are often necessary in order to adequately stage the disease and asses risk factors. The 5-year overall survival rate of patients with malignant melanoma without lymph node involvement can be up to 98% (Schadendorf et al., 2018). Until very recently if distant metastases were detected (Stage IV) the rate dropped to 15% and a median survival rate of 6 to 9 months with chemotherapy (Diamantopoulos et al., 2016). The only therapy option for patients diagnosed with a stage IV malignant melanoma consisted of systemic chemotherapy with Dacarbazine, a cytostatic agent. The response rate was estimated to be around 10% with no given proof of an effect on overall survival. Newer chemotherapeutic agents like Temozolomide and Fotemustine also did not achieve higher overall survival rates but seemed to be more effective against brain metastases (Perera et al., 2013). With increasing knowledge of the different molecular mechanisms leading to transformation of melanocytes several new therapeutic options have emerged in the past years including molecular targeted therapies and immunotherapies, the latter being described further below.

Discovery of mutations affecting the *BRAF* and *NRAS* genes and their role in cell growth and survival led to the development of targeted therapy with specific inhibitors. Vemurafenib and Dabrafenib, approved for treatment of advanced disease, are inhibitors of the oncogenic *BRAF* kinase and as such have a high specificity for the cells affected by the $BRAF^{V600E}$ mutation. Both are linked to a limited display of patient side effects however. Besides diverse non-skin related side effects one major side effect observed was the development of Squamous cell carcinoma (SCC) in around 22% of patients treated with *BRAF* inhibitors (Hatzivassiliou et al., 2010). Non the less Vemurafenib achieved overall response rates of 53% with a median response duration of 6.7 months (Sosman et al., 2012) and randomized phase III clinical trials suggested significantly improved progression-free survival (PFS) rates on either *BRAF* inhibitor when compared to systemic chemotherapy alone (Hauschild et al., 2012). Due to the fact that most melanomas develop resistance to *BRAF* inhibitors by acquiring alternate oncogenic pathway activation after several months of treatment, further strategies emerged

(Flaherty et al., 2012).

The inhibitors Trametinib and Cobimetinib target MEK, a protein further downstream of *BRAF* in the MAPK pathway. In combination with classic $BRAF^{V600E}$ inhibitors, treatment showed significantly improved overall survival (72% in combination therapy, 65% in monotherapy) after 12 months and median PFS (11,4 months in combination therapy, 7,3 months in monotherapy) in previously untreated patients, without increased overall toxicity, in contrast to Vemurafenib monotherapy (Robert et al., 2015). Recent numbers of the two available combinational therapies with Vemurafenib and Cobimetinib or Dabrafenib and Trametinib even state a median overall survival in patients with stage IV melanoma either untreated or treated with *BRAF* inhibitor and MEK inhibitor between 22−25 months, with 40% reaching an overall survival of 3-5 years (Schadendorf et al., 2018). Nevertheless, acquired resistance against targeted therapy and patients with *BRAF* wild-type melanoma remain a problem.

In a retrospective study, Tietze et al. found that it could be promising to re-challenge patients with a new *BRAF* inhibitor following resistance to another *BRAF* inhibitor and exploitation of all other therapy options. Re-introducing *BRAF* inhibitors despite previous progression under *BRAF* inhibition led to disease control in over 50% of the cases. The Disease control rate (DCR) after re-challenge was 57%, with 8% complete response (CR), 20% partial response (PR) and 28% stable disease (SD). The time that had passed between the earlier treatment and the re-introduction did not seem to play a decisive role nor did other treatments received in this interval (Tietze et al., 2018).

Besides the RAS/RAF/MEK/ERK pathway the PI3K/AKT pathway has been a field of interest in targeted melanoma therapy due to several cross-interactions, reciprocal feedback regulation and common downstream proteins between the two pathways. The high levels of cross-inhibition between the two pathways is shown when blocking one of the pathways promotes the activity of the other (Mendoza et al. 2011). For instance, RAS can activate PI3K and its cascade, or the inhibition of PI3K, or other downstream molecules of the PI3K/AKT pathway, can lead to higher phosphorylation of ERK. AKT negatively regulates ERK activation by phosphorylation of inhibitory sites in Raf kinase. *In vitro* knockdown of AKT in human melanoma cells led to a higher sensitivity to Selumetinib (MEK-inhibitor) showing that the inhibition of the PI3K/AKT pathway sensitizes melanoma cells to MEK-

inhibitors (Grazia et al., 2014; Mendoza et al., 2011). Cells showing resistance to *BRAF* inhibitors and MEK inhibitors responded to AKT pathway inhibitors *in vitro* (Atefi et al., 2011; Greger et al., 2012). This interplay shows that melanoma cells can switch signaling pathways in order to evade therapy and can both positively and negatively regulate each other. Pre-clinical testing on dual blockade of both pathways is an effort to decrease resistance mechanisms, compared to a more classic approach with the targeting of several molecules of the same cascade known as “vertical targeting”.

In terms of vertical targeting, Werzowa et al. showed among others that combined inhibition of PI3K (PI-103) and mTOR (Rapamycin) can lead to cell cycle arrest and induced apoptosis *in vitro* and reduction of tumor volume in a xenograft mouse model (Werzowa et al., 2011).

Dual blockade of both pathways has shown promising results mainly *in vitro* and in pre-clinical trials so far. Clinical trials on the safety and efficacy of combined MEK- and mTOR/PI3K-inhibition combination could not replicate the promising pre-clinical results however and obtained disappointing results (Grazia et al., 2014), mostly due to the vast clinical side effects caused by dual therapy and the not yet fully understood, cross-talk interactions between the two pathways. A clinical phase Ib trial in patients with solid tumors with Trametinib and Everolimus (mTor inhibitor) did not reach phase II due to substantial clinical toxicity (mostly mucosal inflammation) (Tolcher et al., 2015).

It seems the regulating protein PTEN might play a significant role as a potential selection factor for a combined therapy with RAS/RAF/MEK/ERK and PI3K/AKT pathway inhibitors. Inactivation of PTEN, as mentioned above, positively induces the PI3K/AKT pathway, leading to a vast accumulation of PIP3 which in return increases the phosphorylation and activity levels of AKT. Tests with cell lines stemming from tumors of various histological origin showing PTEN-loss had a more promising tumor growth inhibition, following treatment with Trametinib and Everolimus (mTOR-inhibitor), both *in vitro* and in a xenograft mouse model following combined therapy (Milella et al., 2017). Determining PTEN-loss in melanoma patients might therefore distinguish those susceptible to this type of therapy.

1.5 Cancer immunogenicity

Our immune system's main target is to protect our body from hazardous outer and inner influences. This bares the idea, that there must also be mechanisms of the immune system to help evade the inner threats of malignant cells spreading in the host's body. "Immune surveillance" is the term first used to describe these interactions between the host's immune cells and malignant cells (Burnet, 1957). The concept states that malignant cells express tumor-associated antigens on their cell surface which can be recognized by the immune system helping distinguish between healthy and malignant cells and educing protective immunity (Shurin, 2012). Cancer immune surveillance has since been regarded as an important mechanism of defense against transformed cancer cells, only gaining more support with the discovery of immune deficient patients being more prone to developing cancer than healthy individuals. A systematic review of observational studies on the cancer risk of HIV/AIDS patients and organ recipients compared to the general population showed a highly increased cancer risk in immunodeficient individuals (Oliveira Cobucci et al., 2012). Most of the described cancers originate from oncogenic viruses, however there are also indications on a higher risk of solid cancers, e.g. lung cancer, in AIDS patients compared to the general population (Kirk et al., 2007), as well as the development of malignant melanoma being increased in kidney transplanted patients (Moloney et al., 2006).

Further supporting the existence of an endogenous immune system able to recognize tumor antigens are cases of spontaneous remission in melanoma patients that had not undergone specific immunotherapy (Ferradini et al., 1993). Responsible for these spontaneous regressions but also for a better patient outcome seem to be tumor infiltrating lymphocytes (TILs) recognizing antigens on transformed cells in the tumor microenvironment. This accounts not only for melanoma but also for other solid tumors such as lung cancer (Al-Shibli et al., 2008; Tuthill et al., 2002).

The introduction of medical therapy blocking immune-inhibitory signals on immune cells leading to a significant remission in a subset of cancer patients further attest the existence of immune cells detecting and reacting to malignant cells (Redman et al., 2016).

However, even in fully immune competent hosts possessing an intact innate and adaptive immune system tumor cells can still develop. This led to the "cancer

immune-editing" theory, in which three different steps of cancer development have been proposed, namely *elimination*, *equilibrium* and *escape*. In the phase of elimination, transformed cells are identified and destroyed by the immune system. The cells that manage to survive immune destruction enter an equilibrium phase that is dominated by the balance of tumor eliminating/tumor promoting mechanisms and ultimately leads to tumor escape. The escape phase represents the third and final phase of the process, where "immunoedited" tumors begin to grow progressively, become clinically apparent and establish an immunosuppressive tumor microenvironment (Mittal et al., 2014).

1.6 CD4+ T-Cells in anti-melanoma immune responses

Malignant transformation generally results in uncontrolled proliferation of the affected cells leading to stress and inflammation in the affected organism at the latest once cells start growing invasively. The human body reacts to these inflammatory signals with the transmission of cells stemming from the innate, such as Natural Killer Cells and macrophages, and adaptive immune system. CD4+ and CD8+ T-cells belong to the adaptive immune system which helps identify and control nascent tumor cells in a process called cancer immune surveillance (Vesely & Schreiber, 2013).

Naïve CD4+ T-cells develop in the thymus and are activated in the periphery once their T-cell receptor (TCR) binds to cognate Major Histocompatibility Complex II (MHC-II) antigen complexes on professional antigen presenting cells (pAPCs). MHC-II is usually expressed on pAPCs to which e.g. macrophages, B-lymphocytes and dendritic cells belong (Glimcher & Kara, 1992). These pAPCs process exogenous antigens and present them on their cell surface via MHC-II molecules. Once naïve CD4+ T-cells recognize a presented antigen with their TCR the activated T-cell expresses Interleukin 2 (IL-2) and clonally expands, differentiating into so called T helper (Th)-cells. Depending on the types of cytokines involved during the differentiation process CD4+ T-cells turn into different subsets of Th-cells such as Th-1 or Th-2 cells (O'Garra & Arai, 2000). Of these two predominant subsets, Th-1 cells are considered to play the larger role in immune system surveillance of cancerous cells as they are characterized by their secretion of

Interferon-γ (IFN-γ) and Tumor Necrosis Factor α (TNFα). Both cytokines have direct anti-tumor effects and are important for the development and recruitment of cytotoxic T-cells (CTLs) a subset of CD8+ T-cells that eliminate cancer cells. Additionally, Th-1 cells activate pAPCs and furthermore induce the production of antibodies that augment the uptake of tumor cells into pAPCs (Knutson & Disis, 2005). Also, IFN-γ induces additional MHC-II expression on tumor and immune cells at the tumor site generating an immunogenic tumor environment. With reduced or absent melanoma MHC-I expression in many advanced melanoma patients (up to 40% of advanced melanoma cells seem to downregulate their expression of MHC-I), MHC class II–regulated effector CD4+ T-cells might have a much more important role in tumoricidal function than previously assumed (Rodig et al., 2018).

1.7 MHC-II function and expression

As mentioned above MHC-II is essential in the stimulation of CD4+ T-cells and primarily expressed by pAPCs. While MHC-I molecules are expressed ubiquitously, with only a few exceptions (e.g. erythrocytes) and present cytosolic peptides, MHC-II molecules mainly present peptides from endocytosed proteins that have been degraded in the endocytic pathway.

A MHC-II molecule consists of two glycoprotein subunits (α and β), these two form a peptide binding groove from where processed peptides can be presented to CD4+ T-cells. In order to recognize and present a vast amount of pathogenic antigens it is crucial that MHC-II molecules can bind as many peptides as possible. In humans, various types of polymorphic MHC-II molecules are encoded by the so called human leukocytes antigen (HLA) gene complex located on chromosome 6 (consisting of HLA-DR, -DP and -DQ) providing a high spectrum of possible peptide binding motifs. The MHC-II proteins combine to form heterodimeric (αβ) protein receptors, therefore speaking of MHC-II can generally be regarded as synonymic for HLA-DR, -DP and -DQ (HLA class II). Additionally MHC-II polymorphism within populations leads to diverse peptide-binding motifs which further increases the recognition of exogenous antigens (ten Broeke et al., 2013).

MHC-II molecules are assembled in the endoplasmic reticulum (ER) and associated with an invariant chain (Ii) called CD74, its presence is linked to the expression of

MHC-II proteins on the surface of cells (Su et al., 2017). CD74 serves as a chaperone and prevents premature loading of the MHC-II binding site, it is a non-polymorphic type II transmembrane glycoprotein. The Ii-MHC-II complex is transported to the MHC-II compartment (MIIC) where CD74 is “clipped” from the binding site and exchanged for a specific peptide that has been processed from a protein in the endocytic pathway. The MHC-II complex is then transported to the surface of the membrane where it can present itself to CD4+ T-cells (Neefjes et al., 2011).

On the molecular level, MHC-II (and also CD74) expression depends on its transcriptional regulator Class II transactivator (*CIITA*). Overall there are a total of four described tissue-specific promoters operating the expression of *CIITA*, whereof promoter I is active in DCs, promoter III is typical for B cells and promoter IV is inducible by IFN-γ (Krawczyk et al., 2006; Scharer et al., 2015).

1.8 MHC-II expression in melanoma

As mentioned, MHC-II expression is normally restricted to a subset of APCs such as dendritic cells, B-cells and macrophages. However, upon stimulation with IFN-γ most cells are capable of expressing MHC-II de novo (Steimle et al., 1994).

In melanoma cell lines, different patterns of MHC-II expression have been described. An IFN-γ dependent stimulation regularly leads to HLA-DR and HLA-DP expression, mostly lacking HLA-DQ (Rodríguez et al., 2007). IFN-γ binds to its receptor leading to the dimerization of two separate IFN-γ receptors. Cross-phosphorylation allows binding of the Janus kinases (JAK) 1 and JAK2 and upon further phosphorylation JAK1 and JAK2 bind signal transducer and activator of transcription 1 (STAT1). Phosphorylated STAT1 forms the homodimer γ-activated factor (GAF) which shifts to the nucleus, where it binds the γ-activation sequence (GAS) on the promoters of the interferon response elements (IRF) 1 and IRF2. The IRF1 and IRF2 heterodimer along with GAF binds promoter IV of *CIITA*. To complete MHC-II transcription *CIITA* binds to an enhanceosome complex. The enhanceosome consists of regulatory factor X (RFX), nuclear factor Y (NFY) and cAMP regulatory element binding protein (CREB). After binding of *CIITA* to the enhanceosome RNA polymerase II can transcribe MHC-II (Osborn et al., 2015).

Constitutive HLA class II expression, which is regularly independent of IFN-γ, is linked to a constitutive expression of *CIITA*. A constitutive transcription of *CIITA* from promoter III was shown in melanoma cells constitutively expressing MHC-II. Responsible might be an enhancer upstream of this promoter III (Deffrennes et al., 2001). The MAPK pathway that is most frequently deregulated in melanoma cells might play a role in the activation of *CIITA* expression, in combination with Activating Protein-1 (AP-1) acting on an Activating Protein-1-responsive element in pIII of the *CIITA* gene (Martins et al., 2007). AP-1 is a collective term referring to dimeric transcription factors that bind to a common DNA site, the AP-1-binding site, involved in functions such as cell proliferation and survival (Karin et al., 1997).

MHC-II expression is seen in melanoma metastases, however the activation of constitutive MHC-II expression is possibly a very early event in melanoma development as studies showed that melanoma cells of primary tumors constitutively expressed MHC-II months before it was also detected in metastases of the same primary tumor (Donia et al., 2015).

Johnson et al. postulated that while IFN-y induces HLA-DR expression there must also be a tumor-cell autonomous inflammatory signal present in the subset of melanoma cells that show constitutive expression of HLA-DR regardless of any IFN-y stimulation. Bioinformatics showed gene-expression pathways upregulated in melanoma cell lines expressing MHC-II suggestive of the presence of an inflammatory signature (Johnson et al., 2016). Furthermore, resistance to IFN-y stimulated HLA-DR expression may be related to Signal transducer and activator of transcription 5 (STAT5) as Johnson et al. observed it was consistently upregulated in constitutively HLA-DR negative melanoma cells indicating resistance to interferon signaling.

Wellbrock et al. described that STAT5 expression is common for pigment cells of the epidermis however the number of STAT5-expressing cells is significantly higher in neoplastic lesions compared to benign nevi and often overexpressed in advanced melanoma cell lines resistant to anti-tumor effects of interferon signaling. STAT5 overexpression and activation counteracts growth inhibition by interfering with STAT1-activation which is necessary for MHC-II transcription and antiproliferative actions and instead induces mitogenic and antiapoptotic signaling (Wellbrock et al., 2005).

1.9 Current advancements in melanoma immunotherapy

As previously described, T-cell activation depends on the presentation of molecules via MHC in order for their TCR to recognize a specific antigen. The presentation of antigens by a professional APC to naïve T cells requires at least two signals. First of all, the interaction of the MHC/Ag complex with the TCR sends an activating signal to the T-cells followed by a second signal that results from the interaction of so called B7 molecules (CD80 and CD86) on the APC with the CD28 stimulatory receptor expressed on T-cells. Co-stimulation by ligation of the co-receptor CD28 on T-cells by B7 molecules on APCs is necessary for optimal T-cell activation. These two signals lead to the activation of CD4 (through MHC-II) and CD8 (through MHC-I) T-cells. Once activated, Cytotoxic T-lymphocyte antigen-4 (CTLA-4) as well as PD-1 are eventually upregulated on the T-cell surface, these receptors bind to B7 molecules and the ligand of PD-1, PD-L1, with high affinity and induce T-cell exhaustion and apoptosis in order to prevent Cytotoxic T-cell (CTL) over-reactivity (de Charette et al., 2016; Linsley et al., 1991).

An encouraging approach to melanoma therapy is that of immune checkpoint inhibition. It has been shown that tumor cells can express intrinsic levels of PD-1 on their own cell surface in order to evade CTL immune effect and promote tumorigenesis (Zhang et al., 2019). Ipilimumab, Tremelimumab (anti-CTLA-4), Pembrolizumab, Nivolumab (anti-PD-1) and Avelumab (anti PD-L1) are monoclonal antibodies that block their respective receptors initializing a more effective CTL immune response. These antibodies have been approved by the FDA and are currently applied for patients with advanced melanoma, with the exception of Avelumab which is currently only approved for treatment of Merkel cell carcinoma (Webb et al., 2018). A combined therapy consisting of both CTLA-4 and PD-1 inhibitors has shown to be more effective than a monotherapy of either inhibitor alone (Rodig et al., 2018), reason being that anti-CTLA-4 mainly targets circulating T-cells and anti-PD-1 targets tumor infiltrated T-cells (Zhang et al., 2019). A combined therapy consisting of Ipilimumab and Nivolumab in untreated melanoma patients led to a median progression free survival of 11,5 months, compared to 2,9 months with Ipilimumab and 6,9 months with Nivolumab monotherapy (Larkin et al., 2015).

In terms of further melanoma treatment options, recent research has focused upon

identifying the specific antigens behind tumor cell recognition in addition to understanding MHC expression in melanoma in order to optimize the immune system's answer to transformed cells. Tumor antigens recognized by the immune system can be categorized into the following groups: *Differentiation antigens*, *oncofetal antigens*, *overexpressed antigens* and *mutated*/*tumor specific antigens (neoantigens)*.

Differentiation antigens are expressed during the development of cells which means that their lacking or decreased expression can be a sign of cell de-differentiation (Tanaka et al., 2011). Melanocyte differentiation antigens (MDA) are expressed by melanocytes that have completed melanogenesis, meaning they have differentiated from melanoblasts (precursor cells of melanocytes that originate from embryonic neural crest cells) into functional melanocytes that have taken up the production of melanin pigments mainly in the skin, eyes and hair. The main function of melanin is to protect neighboring keratinocytes from UV-induced damage (D'Mello et al., 2016). The loss of differentiation is a key feature for tumor cells and in melanoma patients' alterations of several differentiation antigens that play important roles in melanin synthesis have been described, including Melan-A or Tyrosinase. All mentioned MDAs depend on MITF as a transcription regulator showing its key role in melanogenesis and how a downregulation can alter melanocyte differentiation (D'Mello et al., 2016). Understanding the activating mechanisms behind de-differentiation of MDAs is of high clinical relevance in order to understand and develop antigen-specific therapies for melanoma immunotherapy. Interestingly, in addition to its effect on tumor cell growth and survival, *BRAF* mutation also seems to affect the expression of MDAs. Following treatment with Vemurafenib, Donia et al. observed an increase in MDA expression and an improvement in T-lymphocyte recognition (Donia et al., 2012). A more recent study showed, that upregulation of MDAs and T-lymphocyte recognition depends on the duration of the BRAFi-treatment: Short-term treated tumor cells efficiently activate the pre-existing TIL repertoire, whereas long-term inhibition decreased T-cell activation (Pieper et al., 2018). These findings further imply the importance of exploring treatment combinations such as kinase-targeted therapy with immunotherapy, in order to minimize the effects of treatment resistance.

Another promising treatment method is that of adoptive T-cell transfer (ACT), which is currently being used in clinical trials for patients with advanced melanoma. TILs

are extracted from the patient's tumor, expanded ex vivo and reintroduced into the host, assuming the expanded TILs are potent anti-tumor effectors that have recognized and interacted with MDA bearing tumor cells. While there have been cases of induced durable regression in a subset of patients, limitations are still to be found in the short life span of ex vivo cultivated T-cells as well as the downregulation of MDAs by advanced de-differentiated melanoma cells as an escape mechanism in advanced tumor cells (Lee et al., 2016). Also, most strategies have primarily focused CD8+ T-cells or bulk T-cells for treatment. With the knowledge of the importance of CD4+ T-cells in anti-melanoma response growing however, there have been other strategies aking another approach. Hunder et al. achieved durable clinical remission in a patient with refractory metastatic melanoma by developing a treatment where CD4+ T-cells specific for a certain melanoma antigen (NY-ESO-1) were taken from the patient's peripheral blood, cultivated and reinfused into the patient. The CD4+ T-cell clones led to an increase of IFN-y and Interleukin 2 resulting in a more immunogenic tumor environment (Hunder et al., 2008).

Following up on the advancements of ACT was the development of chimeric antigen receptor (CAR) T-cells. These artificially engineered receptors allow T-cells to recognize a specific antigen on tumor cells (Bernatchez et al., 2012). In terms of CD4+ CAR T-cell therapy Lu et al. investigated the effects of intravenously administering high-dose IL-2 together with autologous CD4+ T-cells that had been modified with a specific MHC-II (HLA-DPB*0401) restricted Melanoma-associated-antigen-A3 (MAGE-A3) TCR, into advanced tumor patients. MAGE-A3 is a cancer germline antigen that is frequently expressed by tumor cells and apart from germline-derived tissues rarely found in normal tissue. All patients had undergone previous treatment and had distant metastases at the time of the treatment. Following the applied T-cell therapy one patient showed a complete clinical response and three patients showed objective responses but experienced disease progression after several months. The study was engineered after previous CAR T-cell therapies with MHC-I restricted TCRs targeting MAGE-A3 led to lethal events in patients (Lu et al., 2017).

2 OBJECTIVE

A subset of melanoma cells constitutively expresses HLA (Human Leukocyte Antigen) class II surface molecules presenting antigens to CD4+ T-cells. Among normal cells, HLA class II expression is restricted to professional antigen presenting cells, like dendritic cells. So far, the regulation of constitutive HLA class II expression in melanoma is poorly defined. However, understanding HLA class II expression in tumor cells is of great interest in particular with regard to novel treatment approaches focusing on the killing of melanoma cells by tumor-reactive CD4+ T-cells.

This project studied the role of MAPK and PI3K/AKT signaling pathways in the regulation of HLA class II expression and the association of HLA class II positivity to tumor cell differentiation.

3 MATERIAL AND METHODS

3.1 Material

3.1.1 Reagents, expendable material, equipment and software

Table 1.1: Used reagents

Reagents	Producer, head office, country
Acrylamide-Bis-Solution [30 %]	Bio-Rad Laboratories GmbH, Munich, Germany
Ammonium persulfate	Sigma- Aldrich, St. Louis, USA
Anti-HLA-DR (PC7)	Beckman, California, USA
Anti-HLA-DR MicroBeads	Miltenyi Biotec, Bergisch Gladbach, Germany
Aqua dest.	Braun, Melsungen, Germany
autoMACS Rinsing solution (#130-091-222)	Miltenyi Biotec, Bergisch Gladbach, Germany
β-Mercaptoethanol	Sigma- Aldrich, St. Louis, USA
Bradford-Solution	Sigma- Aldrich, St. Louis, USA
Bovine serum albumin (BSA) [2 mg/ml]	Sigma- Aldrich, St. Louis, USA
Bromphenoleblue	Sigma- Aldrich, St. Louis, USA
Cycloheximide (C7698)	Sigma- Aldrich, St. Louis, USA
Dako REAL Detection System AP/RED Rabbit/Mouse	Agilent, Santa Clara, California
Dimethylsulfoxid (DMSO)	Merck. Kenilworth, USA
EnVisio™ FLEX Antibody Diluent	Dako, Glostrup, Denmark
EnVisio™ FLEX Mini Kit High pH	Dako, Glostrup, Denmark
EnVisio™ FLEX Wash Buffer (20x)	Dako, Glostrup, Denmark
Ethanol [100 %]	Sigma- Aldrich, St. Louis, USA
Fetal Bovine Serum (FBS)	PAA, Brisbane, Australia
FLEX Haematoxylin	Dako, Glostrup, Denmark
Gibco™ Phosphate-Buffered Saline (PBS)	Thermo Fisher Scientific, Waltham, USA
Glycerol	Roth, Newport Beach, USA
Glycin	Roth, Newport Beach, USA
Goat serum # 156046	Abcam, Cambridge, UK
Hydrogen peroxide (H_2O_2) [30 %]	Merck, Darmstadt, Germany
Isopropanol	Merck. Kenilworth, USA
Luminol	Sigma- Aldrich, St. Louis, USA
MACS BSA Stock Solution (#130-091-376)	Miltenyi Biotec, Bergisch Gladbach, Germany

Matrigel growth factor reduced	Corning, New York, USA
Methanol [99 %]	Merck. Kenilworth, USA
Milk powder, Blotting-grade	Roth, Newport Beach, USA
N, N, N´, N´-Tetramethylethylenediamine	Sigma- Aldrich, St. Louis, USA
PageRuler™ Prestained Protein Ladder	Fermentas, Burlington Ontario, USA
Paraformaldehyde (PFA) [4 %]	Sigma- Aldrich, St. Louis, USA
Ponceau-Solution	Sigma- Aldrich, St. Louis, USA
Propidium iodide	BD Pharmingen, Alschwill, Germany
Sodium chloride	Merck. Kenilworth, USA
Sodium Dodecyl Sulphate (SDS)	Gerbu, Heidelberg, Germany
Taq-DNA- Polymerase	Bio-Rad Laboratories GmbH, Munich, Germany
Taqman Universal PCR Mastermix	Applied Biosystems, Foster City, USA
Tris (Trizma Base)	AppliChem, Darmstadt, Germany
Tris-HCl (Trizma Hydrochloride)	Sigma- Aldrich, St. Louis, USA
Triton-X-100	Gerbu, Heidelberg, Germany
Trypanblue [0.5 %]	Biochrom, Cambourne, UK
Tween 20	Gerbu, Heidelberg, Germany

Table 1.2: Used primary antibodies for Western Blot

Primary Antibody	Specificity	Size of the detected protein [kDa]	Producer, head office, country
AKT	Rabbit pAB #9272	60	Cell Signaling, Danvers, USA
pAKT	Rabbit mAB #4060	60	Cell Signaling, Danvers, USA
ERK 1/2	Rabbit polyclonal AB (pAB) #9102	42, 44	Cell Signaling, Danvers, USA
pERK 1/2	Rabbit monoclonal AB (mAB) #4376	42, 44	Cell Signaling, Danvers, USA
GAPDH	Rabbit mAB #2118	37	Cell Signaling, Danvers, USA
MelanA	Mouse mAB # MSK056	20 – 24	Zytomed, Berlin, Germany
MITF	Mouse mAB # 56725	50 – 70	Sigma-Aldrich, Saint Louis, USA

MHC-II (HLA-DR, - DP, - DQ)	Mouse mAB LGII-612.14	25-35	Soldano Ferrone
p53	Rabbit pAB #9282	53	Cell Signaling, Danvers, USA

Table 1.3: Used secondary antibodies for Western Blot

Secondary Antibody	Specificity	Producer, head office, country
Anti-mouse IgG, Horseradish Peroxidase linked	Polyclonal AB anti-Mouse #7076	Cell Signaling, Danva, USA
Anti-rabbit IgG, Horseradish Peroxidase linked	Polyclonal AB anti-rabbit #7074	Cell Signaling, Danva, USA

Table 1.4: Used Taqman-probes

Target gene	Reference Applied Biosystems	Quencher
GAPDH	Hs99999905_m1	FAM/MGB
ß-Actin	Hs99999903_m1	FAM/MGB
HLA-DRA	Hs00219575_m1	FAM/MGB
CIITA	Hs00172106_m1	FAM/MGB
CD74	Hs00269961_m1	FAM/MGB

Table 1.5: Used primary antibodies for immunocytochemistry

Primary antibody	Specificity	Origin
MHC-II (HLA-DR, - DP, - DQ)	Mouse mAB LGII- 612.14	Soldano Ferrone

Table 1.6: Used cell lines

Cell line	Origin	Source
Ma-Mel-61a	Human melanoma cell line	Department of Dermatology,

		University Hospital Essen (UHE)
Ma-Mel-61b	Human melanoma cell line	Department of Dermatology, UHE
Ma-Mel-86b	Human melanoma cell line	Department of Dermatology, UHE
Ma-Mel-86c	Human melanoma cell line	Department of Dermatology, UHE

Table 1.7: Used inhibitors

GSK2110183 2 (2 µM) (1047644-62-1)	Pan-AKT inhibitor	Selleck Chemicals, Houston, USA
PLX-4032 (1 µM) (918504-65-1)	BRAF-V600E/K-specific MAPK pathway inhibitor	Selleck Chemicals, Houston, USA

Table 1.8: Expendable material

Expendable material	**Producer, head office, country**
3 MM Chromatographie-Paper, Whatman®46x57cm	GE Healthcare, Little Chalfont, UK
6-, 24-Well Cell Culture Plate	Greiner Bio-One GmbH, Essen, Germany
96-Well Cell Culture Plate, sterile, flat-bottom, with lid	Greiner Bio-One GmbH, Essen, Germany
Amersham™ Hybond™-ECL	GE Healthcare, Little Chalfont, UK
Amersham™ Hyperfilm™ ECL 18x24 cm	GE Healthcare, Little Chalfont, UK
Blotting paper cards cytospin	Thermo Fisher Scientific, Waltham, USA
Cell culture flasks CELLSTAR® 75 cm^2; 175 cm^2	Greiner Bio-One GmbH, Essen, Germany
Cell lifter, 28 cm	Greiner Bio-One GmbH, Essen, Germany
Coverslip	Neubauer, Erlen, Schwitzerland
Cover slips, round Ø 10 mm	Neolab, Heidelberg, Germany
Cryo-freezing tank	Sigma- Aldrich, St. Louis, USA
Cryo-Vials 2 ml	Greiner Bio-One GmbH, Essen, Germany
Eukitt	Sigma- Aldrich, St. Louis, USA
FACS tubes	Beckman Coulter, San Diego, USA

Filter, 0.2 µm steril	Sartorius, Göttingen, Germany
Glas pipettes 5 ml, 10 ml, 20 ml	Hirschmann® EM Techcolor, Eberstadt, Germany
Gloves	Hartmann, Wiener Neudorf, Austria
Microscope slide	Engelbrecht, Edermünde, Germany
Neubauer-counting chamber	BRAND, Wertheim, Germany
Optical-Adhesive-Covers	Applied Biosystems, Foster City, USA
Pasteurpipettes, non-steril	Oehmen Laborbedarf, Essen, Germany
Petridishes 100/20 mm; 60/12 mm TC Greiner	Greiner Bio-One GmbH, Essen, Germany
Pipette tips 20, 200, 1,000 µl	Rainin Instrument LLC, Oakland, USA
Pipette plugin cotton	Oehmen Laborbedarf, Essen, Germany
Plastic pipettes CELLSTAR® 5 ml, 10 ml, 25 ml	Greiner Bio-One GmbH, Essen, Germany
PP CELLSTAR® tubes 15 ml, 50 ml	Greiner Bio-One GmbH, Essen, Germany
Reaction tubes 0.5 ml, 1.5 ml, 2 ml	Eppendorf, Hamburg, Germany
Xylol	

Table 1.9: Used equipment

Equipment	**Producer, head office, country**
Assembly tool	Acea Bioscience, San Diego, USA
Autoclave (VX-95)	Systec GmbH, Linden, Germany
<u>Centrifuges:</u> Biofuge pico Multifuge 3 S-R Rotanta 460R Microliter centrifuge Z 216 MK	 Hereaus Instruments, Hanau, Germany Thermo Fisher Scientific, Waltham, USA Hettich Zentrifugen, Mülheim an der Ruhr, Germany Hermle Labortechnik GmbH, Wehingen, Germany
CIM plate 16	Acea Bioscience, San Diego, USA
CO_2-Incubator	Binder GmbH, Tuttlingen, Germany
Concentration measurement (Infinite M200)	Tecan Group Ltd. , Männedorf, Switzerland
DAKO Autostainer link 48	Agilent, Santa Clara, California

DNA Thermalcycler (Peqstar 2x gradient)	PEQLAB, Erlangen, Germany
Enduro Power Supplies	Bio-Rad Laboratories GmbH, Munich, Germany
Film-develop cassette	Bio-Rad Laboratories GmbH, München, Germany
Flow cytometer (Gallios)	Beckman Coulter, California, USA
Fully automated Pipettecleaner (PSD)	Hölzel, Cologne, Germany
Icemachine (AF-200)	Scotsman Ice Systems, Milan, Italy
Magnet stirrer (Combimag RCT)	IKA, Staufen, Germany
Micro pipettes 10 µl, 200 µl, 1,000 µl (LTS)	Rainin Instrument LLC, Oakland, USA
Microscope (DMLS)	Leica Biosystems LTD, Newcastle upon Tyne, UK
Microwave (MW 700)	Severin, Sundern, Germany
MidiMACS cell separator + LS column	Miltenyi Biotec, Bergisch Gladbach, Germany
Mini Trans-Blot Cell Vertical-Electrophoresis-System	Bio-Rad Laboratories GmbH, Munich, Germany
Multichannel pipette	Rainin Instrument LLC, Oakland, USA
Nanodrop 2000	Thermo Fisher Scientific, Waltham, USA
PCR-Station (Ultraviolet Sterilizing PCR Workstation)	PEQLAB, Erlangen, Germany
pH-Measurement (pH 510 CyberScan)	Eutech Instruments, Nijkerk, Netherlands
Pipetboy (FASTPETTE V-2)	Lab'Net, Dülmen, Germany
Quantitative PCR	Step One Plus Real- time PCR system (Applied Biosystems), Foster City, USA
Roller (TRM 50)	IDL GmbH & Co, KG, Niederau, Germany
Scale (ALJ 220-5DNM & EW6000-1M)	Kern & Sohn GmbH, Balingen, Germany
Thermomix	Eppendorf, Hamburg, Germany
Vortex (UZUSIO VTX-3000L)	Laboratory& Medical supplies, New Jersey, USA
Water bath	Fischer & Rintelen, Essen, Germany
xCELLigence	Roche, Basel, Germany

Table 1.10: Used software

Software	Producer, head office, country
Graph Pad Prism	GraphPad Software, San Diego; USA
Image J	Scripps Research Institute, La Jolla; USA
Kaluza Flow Cytometry Analysis v1.2	Beckman Coulter, San Diego, USA
Magellan7	Tecan Group Ltd., Männedorf, Schwitzerland
Microsoft Office	Microsoft, Redmond; USA
RTCA 1.2.1	Acea Bioscience, San Diego, USA
StepOne Software v2.1	Applied Biosystems, Foster City, USA

3.1.2 Used kits

High-Capacity cDNA Reverse Transcription Kit (Applied Biosystems)

RNeasy Plus MiniKit, DNase 1 and RNase-free Set (Qiagen)

Anti-HLA-DR MicroBeads and isolation kit (MACS Miltenyi Biotec)

Dako REAL Detection System AP/RED Rabbit/Mouse (Dako, Agilent Technologies)

3.1.3 Buffer and solutions for cell culture and counting

Trypan blue	3.6 ml trypan blue 6.4 ml 1x PBS
2x trypsin/EDTA:	used for detachment of adherent cells from a flask, 10x trypsin/EDTA was diluted with aqua dest. into 2x
Freezing medium:	90 % Fetal Bovine Serum (FBS) 10 % DMSO
Penicillin/Streptomycin 100x	Penicillin 10.000 U/ml Streptomycin 19 mg/ml
RPMI-1640	This medium contains L-Glutamine and was used, complemented with 10 % FBS and 1 % Penicillin/ Streptomycin, for cultivating eukaryotic cells.

Dulbecco's PBS (DPBS)	To wash cells during preparation and serial transfer NaCl 8000 mg/l KCl 200 mg/l Na_2HPO_4 1150 mg/l KH_2HPO_4 200 mg/l $MgCl_2$ x $6H_2O$ 100 mg/l $CaCl_2$ 100 mg/l

3.1.4 Buffer and solutions for protein isolation and Western Blot

1x cell lysis buffer:	20 mM Tris-HCl [pH 7.5] 150 mM NaCl 1 mM Na_2EDTA 1 mM EGTA 1 % Triton 2.5 mM natrium pyrophosphate 1 mM ß-glycerophosphate 1 mM Na_3VO_4 1 µg/ml leupeptin
10 % SDS:	50 g SDS 500 ml aqua dest.
10 % ammonium persulfate:	1 g ammonium persulfate 10 ml aqua dest.
1.5 M Tris [pH 8.8]:	90.85 g Trizma Base 20 ml 10 % SDS filled up to 500 ml with aqua dest.
1 M Tris [pH 6.8]:	15.15 g Trizma Base 10 ml 10 % SDS filled up to 250 ml with aqua dest.
Separating gel (10 %):	1.9 ml H_2O 1.7 ml 30 % acrylamide mix 1.3 ml 1.5 M Tris [pH 8.8] 0.05 ml 10 % SDS 0.05 ml 10 % ammonium persulfate 0.002 ml TEMED
Stacking gel (5 %):	0.68 ml H_2O 0.17 ml 30 % acrylamide mix 0.13 ml 1 M Tris [pH 6.8] 0.01 ml 10 % SDS 0.01 ml 10 % ammonium persulfate 0.001 ml TEMED
4x Sample buffer:	0.25 M Tris-HCl [pH 6.8]

(Laemmli-buffer)	8 % SDS 40 % glycerin 20 % β-Mercaptoethanol Spattle tip bromphenoleblue
10x running buffer:	60 g Trizma Base 20 g SDS 288 g glycine filled up to 2 l with aqua dest.
10x transfer buffer:	60 g Trizma Base 7.48 g SDS 290 g glycine filled up to 2 l with aqua dest.
0.1 % Tween-20 washing buffer:	200 ml 10x PBS 2 ml Tween-20 filled up to 2 l with aqua dest.
5 % milk:	5 g milk powder 100 ml 0.1 % washing buffer
5 % BSA:	5 g bovine serum albumin 100 ml 0.1% washing buffer
Solution A for Western Blot development :	stored at 4 °C 200 ml 0.1 M Tris-HCl [pH 8.6] 50 mg luminol
Solution B for Western Blot development:	stored, light protected, at RT 11 mg para-hydroxycoumarinsäure 10 ml dimethylsulfoxid
ECL-Detection reagent:	4 ml Solution A 1.2 µl 30 % H_2O_2 400 µl Solution B

3.2 Methods

3.2.1 Cellular methods

Melanoma cell culture (incl. passaging, counting, cryopreservation)

The adherent cells were held in RPMI 1640 medium containing 10% FBS and 1% Penicillin/Streptomycin (P/S) referred to as culture medium and cultured at 37°C and 5% CO_2.

Cells were passaged on a regular 3-4 day basis with a minimum of 80% confluent cells. In order to do so the used medium was discarded and the cells washed with 1x DPBS. The melanoma cells were then incubated with 1.5-2 ml Trypsin-EDTA for 5 min to remove them from the surface of the culture-flask. After incubation the flask was carefully shaken to fully detach all cells. The cell suspension was then taken up in 10 ml of RPMI 1640 and centrifuged at 1200 rotations/min (rpm) for 7 min to get rid of remaining trypsin. The supernatant was removed and the pellet once again taken up in 10 ml of RPMI 1640. Depending on the cell line 0.5-3 ml of this cell suspension were returned back into a culture flask containing 20 ml of fresh culture medium. The cultivation of the cells was subsequently continued at 37°C and 5% CO_2.

Melanoma cells were frozen down in 1 ml portions. The cells were sedimented (7 min, 1,200 rpm and RT) before being resuspended in freezing medium (FBS + 10% DMSO) and distributed into cryo-vials. Over 24 h the cells were gradually frozen at -80°C before the vials were transferred into a liquid nitrogen tank. To carefully thaw cells, the cryo-vials were put in the incubator (37°C, 5% CO_2) however not completely thawed and then taken up in 10 ml of RPMI 1640 in a 15 ml Falcon tube. Subsequently the cells were centrifuged in order to remove the freezing medium. The pellet was then resuspended with 5 ml of culture medium and added to further 5 ml of medium in a T75 flask. Cultivation was continued at 37°C with 5 % CO_2.

A Neubauer counting chamber was used to determine the cell count. 5-10 µl of the cell suspension were diluted 1:5 or 1:10 with trypan blue, depending on the expected amount of cells in the suspension. The suspension was then pipetted under the cover glass of the Neubauer counting chamber. The trypan blue dyed dead cells blue making it possible to only count the living cells. The cells in 4 quadrants were

counted, an average number of cells calculated and the dilution factor added into the equation: *Average number of cells x dilution factor x 10^4 = Cells/ml*

Cell sorting

Magnet based cell separation was performed to isolate MHC-II expressing melanoma cells from the bulk cell line. The cells were sorted by MACS Miltenyi Biotec Anti-HLA-DR MicroBeads.
Cells were repeatedly washed with DPBS and then detached from the flask in similar fashion to the process used when passaging the cells. Afterwards the cell suspension was centrifuged at 1200 rpm for 7 min. The cells were then resuspended in 400 µl of MACS buffer solution containing PBS, 0.5% bovine serum albumin (BSA), 2 mM EDTA and a dilution of MACS BSA Stock Solution 1:20 with autoMACS Rinsing Solution. Afterwards 100 µl of anti-HLA-DR microbeads were added and the solution was incubated for 15 min at 4°C. Next the cells were washed with 5 ml of buffer and again centrifuged at 1200 rpm for 7 min. The supernatant was aspirated and the cells resuspended into 500 µl of buffer. Simultaneously a Miltenyi Biotec LS column was placed into the magnetic field of a suitable MACS separator and prepared with 3 ml of buffer solution before the cells were applied to the column. The flow-through was collected and the column again washed with buffer solution before the supernatant was reapplied to the column in order to collect remaining labeled cells that were not bound to the magnetic column during the first run. These steps of washing and separation were repeated a total of 3 times. After the third passage the flow-through containing the unlabeled cells was discarded and the column was removed and placed over a suitable collection tube. 5 ml of buffer were pipetted onto the column and immediately a plunger was firmly pressed down washing the HLA-DR positive labeled cells out of the column. The HLA-DR positive cells were then cultured and expanded.

Flow cytometry

Flow cytometry is a method used to detect and quantitatively determine proteins located on the surface of cells as well as intracellular proteins.
To begin with, the adherent melanoma cells were detached from the flask surface via trypsin, centrifuged for 7 min at 1200 rpm followed by the determination of the

cell number. $1x10^5$ cells per treatment were given into a well of a 96 well plate and the supernatant eliminated after centrifugation. Subsequently the pellets were resuspended in 100 µl of Phosphate-Buffered Saline (PBS) and incubated with the appropriate amount of primary antibody (PECy7-labelled anti-HLA-DR) at 4°C for half an h. Afterwards the cells were repeatedly washed with 200 µl of PBS and centrifuged at 1200 rpm for 7 min to again eliminate the supernatant. The treated cells were then taken up in 350 µl of 1xDPBS/ 3,7% formaldehyde, filled into a FACS tube and analyzed using the Gallios flow cytometer. Main focus was set upon the expression of MHC class II (HLA-DR) receptors on the surface of melanoma cells Ma-Mel-86b, Ma-Mel-86c and Ma-Mel-61a following AKT-inhibitor and BRAF-inhibitor treatment as well as comparing the base expression rate of MHC-II on the surface of these cell lines.

Invasion assay

The xCELLigence RTCA DP system by ACEA Biosystem was used to study the invasiveness of sorted melanoma cell lines expressing high levels of HLA-DR compared to non-sorted bulk cell lines (referred to as HLA-DR negative).
The xCELLIgence cell invasion and migration (CIM) plates consisted of two chambers, an upper chamber and a lower chamber. The upper chamber had a microporous membrane at the bottom of each well which the cells could migrate through in the course of 96 h. Gold electrodes at the bottom of the wells then detected adherent cells, by measuring electrical impedance caused by the cells that had passed through the gel which was used to imitate a membrane matrix.
Before pipetting the cells into the upper chamber, the bottom of each well had to be coated by the gel separating the cells from the electrodes. The thawing process of the gel had to be very even and slow so that it would not polymerize during the process (overnight at 4°C), afterwards it was mixed 1:40 with RPMI medium supplemented with 0% FBS + 1% P/S (25 µl gel + 975 µl medium). 20 µl of the diluted gel were pipetted into each well and left to incubate for 4 h at 37°C, 5% CO_2. 160 µl of RPMI medium supplemented with 10% FBS + 1% P/S were filled into each well of the lower chamber and then assembled with the upper chamber containing the hardened matrigel. Next, 30 µl of RPMI medium supplemented with 0% FBS + 1% P/S were filled into each well of the upper chamber and a blank was measured.

The cells used in the assay were constantly cultivated in RPMI supplemented with only 2% FBS + 1% P/S (“starving medium”). After 48 h of incubation the HLA-DR pos. and HLA-DR neg. cells were harvested and their cell number determined. 100 µl of RPMI medium supplemented with 0% FBS + 1% P/S containing $1x10^5$ cells were used per well of the upper chamber. Measurements of the electrical impedance across interdigitated microelectrodes integrated at the bottom of the special tissue culture CIM plates took place every 15 min over a time span of 96 h, measuring the invasive migration process of the starved cells through the membrane towards the medium supplemented with 10% FBS. The cells contacted and adhered to the electronic sensors on the underside of the membrane, resulting in an increase of impedance. The increase of impedance correlated to increasing numbers of invading cells on the underside of the membrane. Cell-index values reflecting impedance changes were automatically and continuously recorded by the RTCA DP instrument.

3.2.2 Molecular biological methods

RNA-Isolation and quantification

The “RNeasy plus Mini Kit“ and the “DNase 1, RNase-free set” from Qiagen were used to isolate RNA from cell pellets. All centrifugation steps for the isolation of RNA were performed at 13000 rpm.

Cell pellets were gained by washing the adherent cells with 1x DPBS followed by 1.5-3 ml of 2x Trypsin/EDTA in order to detach the cells from the surface of the culture-flask. After a short period of incubation the loosened cells were taken up in RPMI medium and centrifuged at 1200 rpm. The formed cell pellet was then dissolved in 1x DPBS before a final round of centrifugation. Once these steps were completed, the pellet was ready to be used for the isolation of RNA.

The cell pellet was resuspended in 350 µl of lysis buffer consisting of 10 µl β-Mercaptoethanol per 1ml of RLT-Buffer. The lysate was directly pipetted on the QIA-shredder-column and centrifuged for 2 min. The homogenized lysate was then pipetted on the genomic DNA (gDNA) Eliminator-spin-column and centrifuged for another 30 sec. Afterwards the column was discarded and the augmented RNA resuspended in 350 µl of 70% ethanol. A maximum of 700 µl was filled on to an

RNeasy mini spin column and centrifuged for 15 sec followed by another 15 sec centrifugation step consisting of mixing the RNA with RW1 buffer for washing the membrane-bound RNA. Subsequently the RNA was treated with the DNase-Mix in order to eliminate any remaining genomic DNA and to ensure the RNA remains bound to the column. The DNase-Mix consisted of 12.5 µl of DNase plus 87.5 µl of RDD-Buffer per solution and 100 µl were then pipetted directly on the membrane of the RNeasy mini spin column. The incubation period was 20 min at room temperature followed by the membrane being washed with both RW1- and RPE-Buffer each for 15 sec. After one final washing step with RPE the column was centrifuged by itself in order to dry. To get rid of any buffer remains the RNA was centrifuged for 1 min with 30 µl of RNase-free water and eluded into a new tube.
Determining the concentration of the gained RNA was necessary in order to calculate the needed amount of RNA for the following cDNA synthesis. For measuring, 1 µl of the pure RNA was pipetted onto the photometric sensor of the Nanodrop. The concentration in µg/µl was then photometrically measured at a wave length of 260nm. To determine the purity of the RNA it was essential to determine the ratio of maximum absorption between DNA and proteins (260nm/280nm). The aim was a quotient around 2, the lower the number the higher the contamination of the gained RNA by remainders of DNA and protein. For calibration purposes 1 µl of distilled water was used as a blank solution before beginning to measure the RNA concentration.

cDNA synthesis

The reverse transcription of RNA in cDNA was achieved by using the “High-Capacity cDNA Reverse Transcription Kit“ of Applied Biosystems. cDNA was synthesized from processed RNA and no longer contained introns (non-encoding sections on eukaryotic DNA) since RNA had already undergone splicing. The synthesis of cDNA was performed by the enzyme reverse transcriptase, a RNA-dependent DNA-polymerase. In order to have a maximum of RNA strands transcribed into cDNA random primers were applied. Each synthesis solution was made up of 20 µl consisting of 10 µl RNA solution containing 1 µg RNA (if the previous determination of the RNA concentration generated very low amounts of RNA it was sometimes necessary to adjust the amount of used RNA) and 10 µl of a Master-Mix.

The Master-Mix contained:

- 25x dNTP Mix (100mM) 0.8 µl
- 10x Reverse Transcription-Puffer 2 µl
- Reverse transcriptase 1.0 µl
- RNase Inhibitor 1.0 µl
- 10x Reverse Transcription Random Primer 2.0 µl
- Nuclease-free H_20 3.2 µl

The following thermal cycler-Program was used for the reverse transcription:

1. 25°C - 10 min
2. 37°C - 120 min
3. 85°C - 5 min
4. 4°C - ∞

The obtained cDNA was subsequently used in a Real-Time-PCR or stored at -20°C.

Quantitative Real-Time-PCR (Taqman)

Quantitative Real-Time-PCR (qPCR) is a procedure that multiplies and quantitatively determines the desired PCR-products. Here the Taqman qPCR was applied which aside from Taqman-primers also included Taqman-probes that specifically bind to the desired, to be amplified DNA section (e.g. for this study *HLA-DRA, CD74, CIITA*). Probes are fragments of DNA or RNA that detect and bind to specific DNA fragments within a sample. Primers on the other hand are short strands of DNA or RNA and initiate the polymerase chain reaction by hybridization with single-stranded DNA. Taqman-probes consist of a quencher- and a reporter fluorescent dye and as long as the probe is intact and the fluorophore is in close proximity to the quencher, no fluorescent signal is emitted. During the amplification process the DNA-polymerase encounters the Taqman-probes and due to its exonuclease activity separates quencher- from reporter fluorescent dye leading to a measurable fluorescent signal. The signal depends on the amount of synthesized DNA. A strong signal therefore correlates with a higher amount of DNA synthesis.

There are different quantification methods, with the $\Delta\Delta C_t$-method being the method of choice for the performed experiments. It describes an algorithm for a relative quantification with the C_t-value functioning as the threshold determining the amount of PCR cycles it takes to measure an amplification signal for the first time (Livak et al., 2001). The amount of the amplified target gene can later be standardized to the amount of a reference gene but is also comparable in between differently treated cell lines. GAPDH is relatively stable among different cell lines in terms of its DNA amount and shouldn't be affected by different medication treatments. None the less qPCR is an extremely sensitive procedure and deviations in the stability of the reference gene had to be considered in the analysis of the data.

Each qPCR reaction consisted of a 10 µl volume in a 96 well plate and contained:

- 1 µl cDNA template
- 5 µl 2x TaqMan Universal PCR Master Mix
- 0,5 µl 20x TaqMan Gene Expression Assay Primer
- 3,5 µl H_2O

The following thermocycler-program was used for qPCR:

- 95°C for 10 min — Denaturation
- 95°C for 15 sec — Annealing
- 60°C for 1 min — Extension

(Annealing and Extension: 40x)

Protein isolation and quantification

Two methods were used in order to extract proteins from the cells. Either the cells were directly lysed in their well or protein isolates were extracted from a cell pellet. The lysis buffer used consisted of 1ml 1x Cell Lysis Buffer + 20 µl PMSF 50mM (protease-inhibitor). All cellular lysis steps were performed on ice to maintain an active and stable conformation of the proteins and to prevent protease action. To lyse the cells in their well they were washed with 1 ml of ice cold 1x DPBS and afterwards a corresponding amount of lysis buffer (50 µl per well on a 6 well plate) was evenly distributed on the cell layer and left to incubate on ice for 5 min. Subsequently the cells were collected with the help of a cell scraper and the gained

cell suspension then transferred into a 1,5 ml Eppendorf tube. Using a cannula the cells were resuspended approximately 5 times in order to shear the DNA and afterwards centrifuged for 15 min at 13000 rpm with the temperature set at 4°C. The supernatant was pipetted into a new tube and stored at -80°C.

Gaining protein isolates out of cell pellets was achieved by resuspending the frozen pellet in 50-100 µl of lysis buffer also followed by centrifugation at 13000 rpm for 15 min at 4°C.

In order to determine the concentration of the proteins a standard curve using BSA (2mg/ml) was prepared. The curve contained the following BSA-concentrations in µg/µl: 1.4; 1.2; 1.0; 0.8; 0.6; 0.4; 0.2. From each of the protein isolates 2 µl were used and diluted as follows: 1:5; 1:10; 1:20; 1:40. Aqua dest. was the diluting agent in all cases. 250 µl of Bradford solution (BioRad) were added to each dilution of the standard curve as well as the protein samples and left to incubate for 5 min at RT. Depending on the protein concentration per sample a color change from brown to blue could be observed. By measuring the absorbance at OD_{595}nm the color shift helped determine the protein concentration. A standard curve was generated by plotting the 595 nm absorbance values on the y-axis versus the respective concentration in µg/ml on the x-axis. The sample concentration was then determined by averaging the deviations from the standard curve. The determined concentration was then multiplied by the dilution factor.

Each sample to be analyzed contained 15 µg of protein and complemented with H_2O to reach an end volume of 10 µl. To each sample 2 µl of 4x sample buffer were added which contained the anionic detergent sodium dodecyl sulphate (SDS). SDS is an anionic detergent used to linearize proteins via denaturation of the secondary structure and non-disulphide linked tertiary structures. This imparted a negative charge to the linearized proteins. Subsequently all proteins showed the same amount of negative charge which led to the size of the proteins being the only factor in their migration velocity through the gel. Additionally the sample buffer contained β-Mercaptoethanol to resolve the disulphide bonds. Further tertiary and quaternary structures were destroyed by heating the proteins up to 99°C for 3 min.

Protein gel electrophoresis and Western Blot (incl. quantification of signal intensity)

The obtained protein samples were pipetted into the chambers of a gel consisting of a stacking gel and a subjacent 10% running gel. The electrophoretic separation of the proteins took place in the running gel.
10 µl of the protein samples and 5 µl of a protein marker were applied to the stacking gel, put into an electrophoretic chamber and then left in a 1x running buffer at 100 Volt until the accumulated proteins reached the border between stacking and running gel. The following protein separation occurred at 100-150 Volt for 1-2 h. Electrophoresis applied an electric field, which caused the migration of the negatively charged proteins (coated with SDS) away from the negative electrode and towards the positive electrode hereby separating the proteins depending on their size. The Western-Blot technique allowed an immunochemical characterization of the protein samples by transferring the separated proteins from an acrylamide gel onto a nitrocellulose membrane where they could be detected with specific antibodies.
For the transfer process the acrylamide gel was placed between two perpendicular electrodes via a “Sandwich-technique” (sponge, 3x Whatman-Paper, gel, membrane, 3x Whatman-Paper, sponge). The perpendicular electric current led to the proteins wandering from the gel onto the membrane where they securely remained due to hydrophobic interactions. To check whether or not the proteins were transferred the membranes were washed with Ponceau-red which stained the protein bands.
After the transfer the membranes were cut according to the expected size of the desired protein band and blocked with 5% skimmed milk for 1 h in order to prevent unspecific binding of the primary antibody, followed by 2-3 washing steps with 0,1% PBS/Tween for 5-10 min. The membranes were then incubated in 5 ml of an antibody solution either in 1% BSA or 5% skimmed milk at 4°C overnight.
On the next day the membranes were taken out of the refrigerator and washed three times for 5 min in 0.1% PBS/Tween in order to rid them of any unspecific binding of the primary antibody followed by 1 h of incubation with the fitting secondary antibody at room temperature. Finally the membranes were washed another three times with 0.1% PBS/Tween for 5 min and once with 1x PBS. All used secondary antibodies were coupled with the enzyme Horseraddish-Peroxidase (HRP) which conjugated

to the primary-secondary antibody complex and all membranes were then incubated with a luminol-peroxidase-solution (ECL) for 2 min. Incubating the HRP with the ECL led to a luminescent signal. The oxidation of the substrate caused the emission of light which was made visible by chemiluminescent films. The X-Ray-films were placed on the membranes for 1 sec – 5 min and then developed in a dark room.
Signal intensity of protein bands was measured with ImageJ, an analysis software used for the quantification of visual results. The Western Blots were scanned and uploaded to the software. Next, bands were selected with a marking tool and analyzed, creating a histogram for each individual protein band. A measuring point was set where the histogram began to drop steeply and another where it leveled out again, the selected area was then used to calculate the signal intensity into a numerical value. The numerical value of each protein's signal intensity was divided by the intensity of its GAPDH loading control to decrease the effect of uneven loading.

Cytospin

Cells were detached from the surface of the culture flask with trypsin and then underwent two steps of washing with PBS and centrifugation at 1200 rpm for 7 min. Afterwards the cell number was determined and an aliquot containing $2x10^4$ cells pipetted onto labeled cover slides. Each slide was then carefully mounted with a cardboard filter showcasing a circular opening (surrounding the aliquot), placed into a slot holder and centrifuged at 1500 rpm for 10 min. The filters absorbed the supernatant fluid and left the cells attached to the center of the coverslip in a circular formation. After carefully detaching the cuvette and the paper and examining each slide under the microscope each slide was then cryopreserved for further staining.

Immunocytochemistry

Thin-layer cell preparations, obtained via cytospin, were stained for MHC-II proteins with the indicated primary antibody in combination with a Polymer Kit containing an AP coupled secondary antibody (Dako REAL Detection System AP/RED Rabbit/Mouse) according to the manufacturer's instructions. The following mAb was used: anti-HLA-DR,-DP,-DQ (1:100) antibody LGII-612.14, recognizing a linear epitope expressed on HLA-DR, -DP, and -DQ β chains.

Following the staining the cells were dried and fixated with a series of ethanol (70% 1min (2x), 96% 1min (2x), 100% 1min (2x)) and xylol washes (2x 2min) and a cover glass was attached.

4 RESULTS

4.1 Phenotypical characterization of melanoma cell lines

Along with several other malignant tumors, melanoma cells are known to be able to constitutively express MHC-II proteins on their cell surface. For this study three melanoma cell lines were taken into cultivation that had shown MHC-II expression in previous experiments. The cell lines were established from melanoma metastases of patient Ma-Mel-61 and Ma-Mel-86. Tumor samples from patient Ma-Mel-86 were obtained in years 1.5 (Ma-Mel-86b) and 3 (Ma-Mel-86c) of stage IV disease, Ma-Mel-61a was also obtained from a metastasis of a stage IV melanoma patient.

In immunocytochemistry two of the cell lines Ma-Mel-86b and Ma-Mel-86c were stained with an antibody (mAb) targeting HLA-DR, -DP, -DQ, a MHC-II molecule encoded by human leukocyte antigen gene complexes, to show that there was in fact a small population of MHC-II pos. cells among them (*Fig. 1.1 A*).

Afterwards the cells were sorted using anti-HLA-DR antibody coupled magnetic beads. The beads tagged the cells expressing HLA-DR on their surface with the cell suspension then passed through a column that was placed between a permanent magnetic field hereby separating the HLA-DR pos. cells from the neg. ones. Subsequently the two cell suspensions were taken into culture and analyzed by flow cytometry to verify the sorting had been successful (*Fig. 1.2*).

As shown in *Fig. 1.2 A* there is a small population of cells expressing HLA-DR on their surface in the bulk cell lines of Ma-Mel-86b, -86c and -61a ranging from approximately 1-7%. The magnetic bead sorting managed to achieve a HLA-DR positive population of a minimum of 96% in all cell lines. Accordingly immunocytochemistry also showed a change in the amount of HLA-DR positive cells (*Fig. 1.1 B*) as did FACS analysis which showed a significant change (except for Ma-Mel-86b, where the process of staining of the sorted HLA-DR positive cells was not as successful in one of three experiments) in the amount of HLA-DR surface expression in the cells post-sorting. Following the sorting of the cells from the bulk cell lines the HLA-DR depleted cells will be referred to as HLA-DR negative (HLA-DR neg.) and accordingly the sorted cells as HLA-DR positive (HLA-DR pos.).

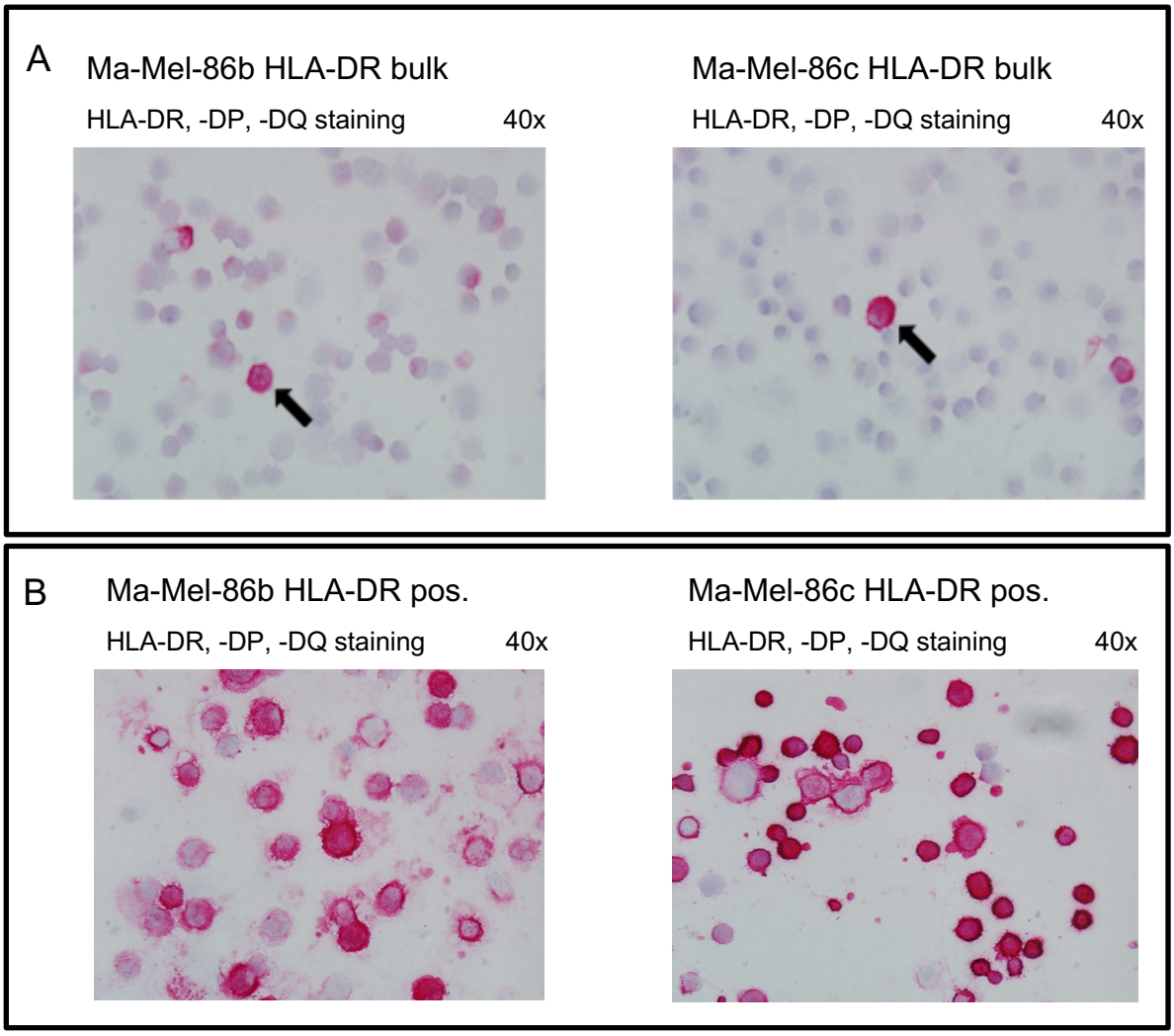

Figure 1.1: Detection of HLA class II expression on melanoma cells by immunocytochemistry

Ma-Mel-86b and Ma-Mel-86c cells were analyzed for the expression of HLA-DR, -DP, -DQ by immunocytochemistry (mAb). Red staining indicates positive cells, arrows pointing at positive cells, 40x magnification. The experiment was performed once for both cell lines pre- and post-staining.

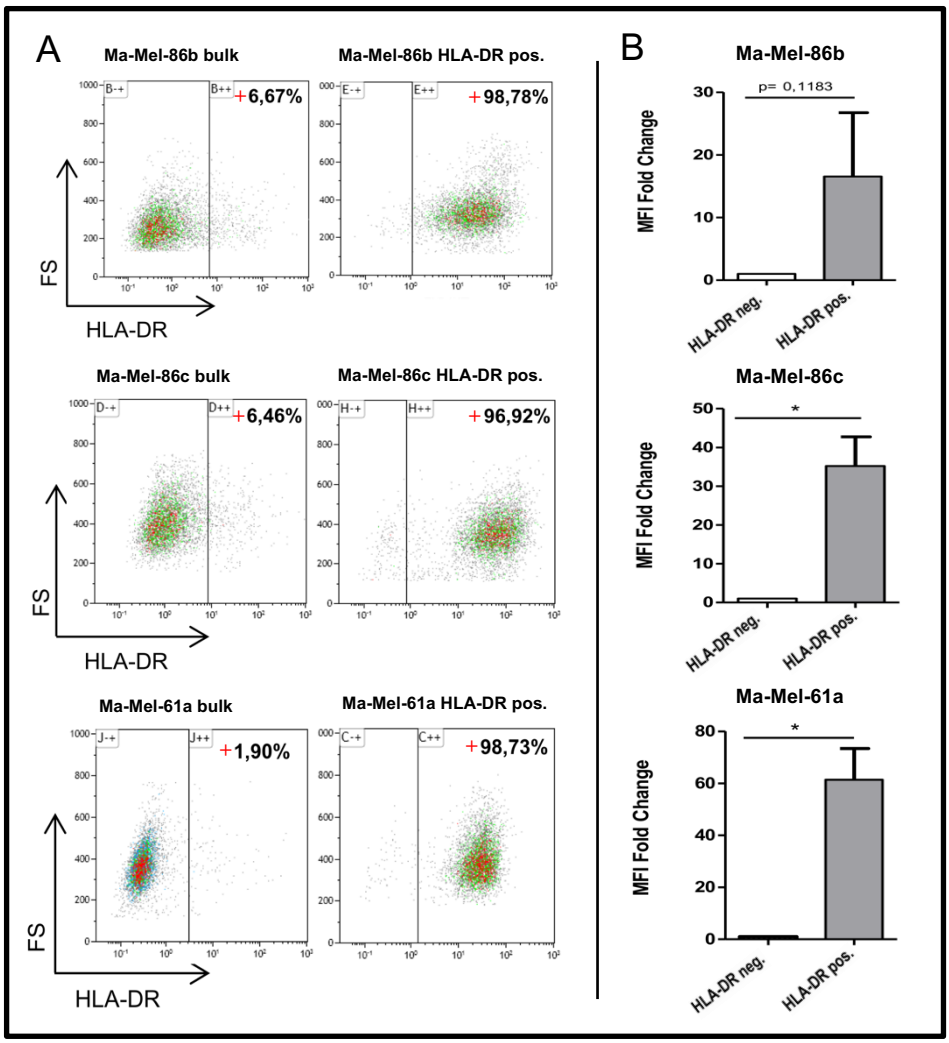

Figure 1.2: Melanoma cell lines show small populations of HLA-DR positive cells in FACS

A) Dot Plots show HLA-DR expression on cell surface of the cell lines Ma-Mel-86b, Ma-Mel-86c and Ma-Mel-61a. The cells were incubated with an antibody (anti–HLA-DR-PECy7) before flow cytometry. Left plots show bulk cell lines with small populations (+) of cells expressing HLA-DR on their surface. The melanoma cells were sorted via magnetic beads and the extracted HLA-DR pos. cells taken into culture. Right plots show HLA-DR pos. cell lines post sorting, as they were used for following experiments. (FS: Forward scatter). One representative of three independent dot plots is shown.

B) Surface expression of HLA-DR on sorted melanoma cells compared to their bulk cell line. HLA-DR surface expression was set to 1 in HLA-DR neg. (corresponding to HLA-DR bulk) cell lines. The values represent mean (± SEM) of at least three independent experiments. Statistically significant differences between HLA-DR pos. and neg. cells calculated by a two-tailed paired student's t-test is shown; stars/horizontal lines mark samples statistically different from the control. (* $p \leq 0.05$).

4.1.1 Analysis of CIITA driven gene expression in melanoma cell subpopulations

To further compare the HLA-DR pos. to the depleted (neg.) melanoma cells data was collected on the mRNA expression levels of not only *HLA-DRA* (the "A" implies the alpha subunit of HLA-DR) but also on *CIITA* and *CD74* (*Fig. 1.3*). *CIITA* is known as the master regulator of HLA-DR and CD74 expression. Levels were therefore expected to be a lot higher in the HLA-DR pos. cell subpopulation which was significantly so in all three cell lines. Correspondingly higher levels of *CD74* were indeed observed in the HLA-DR pos. cell lines.

The observed differences in relative mRNA expression levels of *HLA-DRA*, *CIITA* and *CD74* between the cell lines, especially comparing Ma-Mel-61a to Ma-Mel-86b and -86c are most likely attributed to an initial difference in basic mRNA expression within the three bulk cell lines.

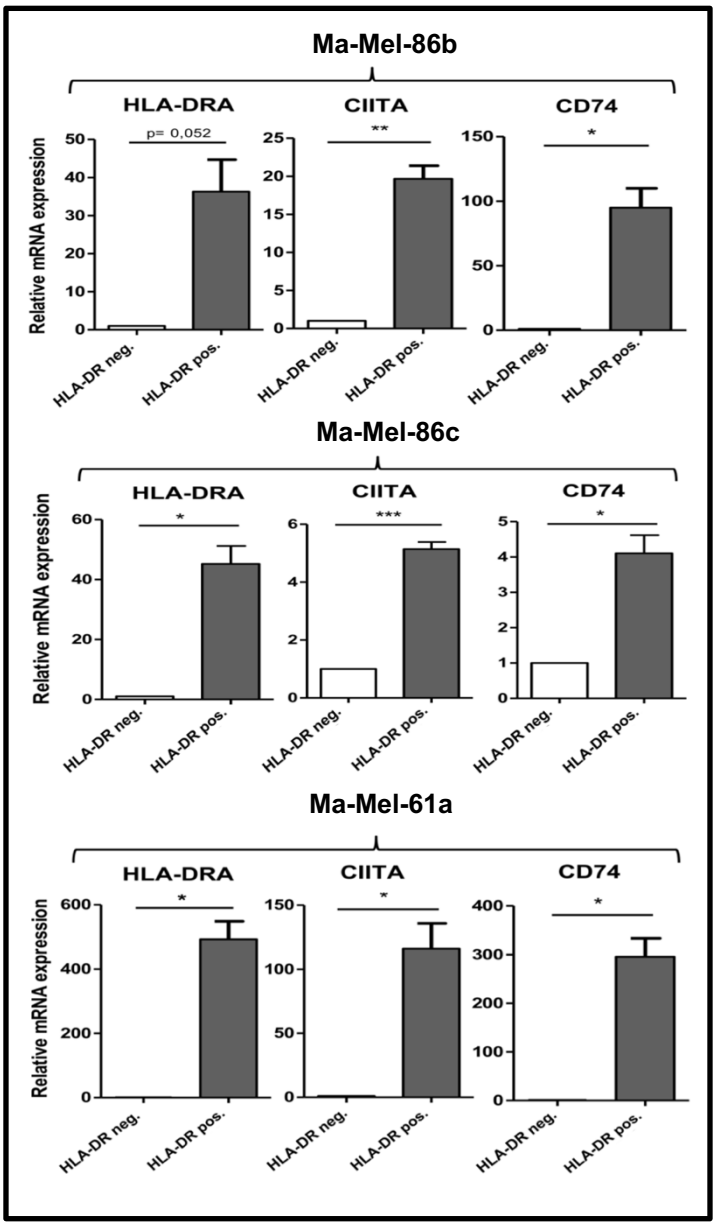

Figure 1.3: HLA-DR positive melanoma cell lines show increased levels of *CIITA* and *CD74*

Comparison of mRNA expression levels in HLA-DR pos. and neg. cell lines. mRNA levels of *HLA-DRA* (alpha subunit of HLA-DR), *CIITA* (master regulator of HLA-DR), *CD74* (invariant chain of MHC-II) in Ma-Mel-86b, Ma-Mel-86c and Ma-Mel-61a cells were quantified by qPCR and normalized to endogenous GAPDH mRNA. The relative mRNA expression levels in HLA-DR neg. cells was set to 1.

Expression levels, given as mean (+ SEM) of three independent experiments. Statistically significant differences between HLA-DR pos. and neg. cells calculated by paired student's t-test is shown; stars/horizontal lines mark samples statistically different from the control (* $p \leq 0.05$, ** $p \leq 0.01$, *** $p \leq 0.005$).

4.1.2 Activation status of signaling cascades related to development of melanoma

The next aim was to compare the activation status of certain signaling cascades in the HLA-DR pos. and HLA-DR neg. cell lines of Ma-Mel-86b, Ma-Mel-86c and Ma-Mel-61a via Western Blot, focusing on proteins involved in the PI3K/AKT and RAS/RAF/MEK/ERK pathway since these two pathways are major factors in the development of melanoma cells. Furthermore the levels of Melan-A and MITF as indicators of cell differentiation were investigated. HLA-DR protein levels were determined to consolidate what had previously been seen on the cell surface of the HLA-DR pos. cells via flow cytometry. GAPDH served as a loading control (*Fig. 1.4.* Full blots of the depicted immunoblots shown in supplementary figures).
While there did not appear to be major differences in basic AKT and ERK levels, pERK levels were noticeably higher in Ma-Mel-86c and -61a HLA-DR pos. cell lines. Ma-Mel-86b also showed higher levels of pERK when comparing the HLA-DR pos. and neg. cells although not as clearly as the other two cell lines. In contrast Ma-Mel-86c and Ma-Mel-61a both appeared to have lower levels of pAKT, the activated form of AKT, in the HLA-DR pos. cell line throughout our tests. Also, both Ma-Mel-86c and -61a HLA-DR pos. cell lines appeared to have noticeably lower levels of melanocyte differentiation antigen Melan-A when compared to the HLA-DR neg. cell lines. Interestingly, Melan-A protein expression levels were rather higher in the HLA-DR pos. cell line of Ma-Mel-86b. In terms of MITF, the transcriptional regulator of Melan-A, Ma-Mel-86c was the only cell line to show the tendency of lower expression levels.

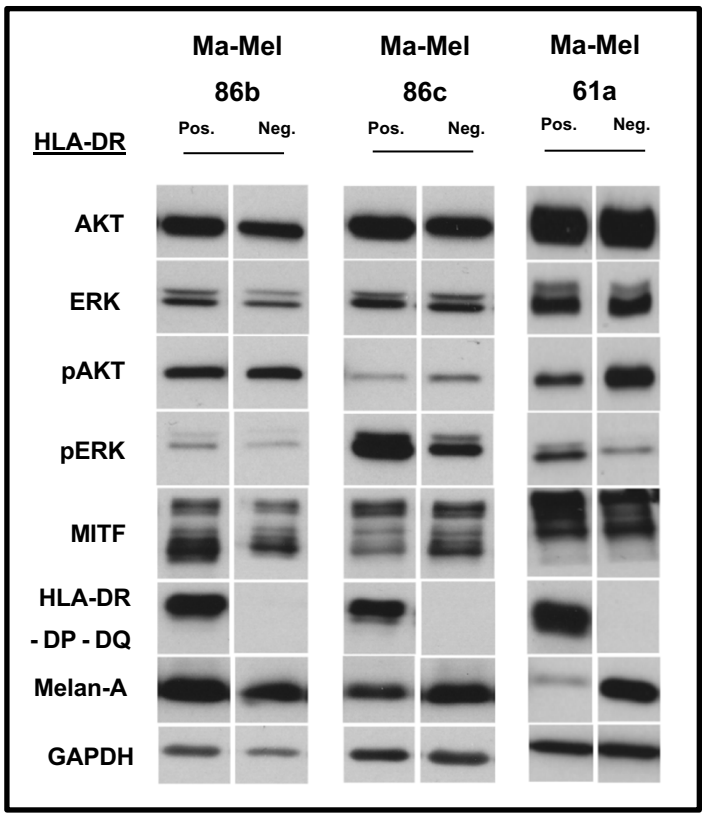

Figure 1.4: HLA-DR positive melanoma cells show higher pERK activation

Cell lysates were analyzed by Western Blot for the protein levels of MAPK and PI3K/AKT pathway components (ERK, AKT, pERK, pAKT), expression of Melan-A and its transcriptional regulator MITF as well as MHC-II (HLA-DR, -DP, -DQ). Expression levels were compared between Ma-Mel-86b, Ma-Mel-86c and Ma-Mel-61a HLA-DR pos. and neg. cells.
GAPDH served as a loading control. Data from one representative of three independent experiments are presented. Due to technical difficulties HLA-DR and Melan-A levels were only determined twice for Ma-Mel-86b and Ma-Mel-86c. Melan-A levels were determined twice for Ma-Mel-61a cells.

4.2 Effect of BRAF inhibition on HLA class II surface expression

Due to the fact that the HLA-DR pos. subpopulation seemed to have higher protein levels of pERK, as seen in *Fig. 1.4*, it was interesting to investigate whether or not there was a link between the RAS/RAF/MEK/ERK pathway and the expression of HLA-DR and which effect it would have if the pathway was blocked. HLA-DR pos. melanoma cells from Ma-Mel-86b and Ma-Mel-86c were incubated with 1 µM of the BRAF-inhibitor (BRAFi) [PLX-4032 (PLX) - Vemurafenib] for 72 h. This procedure was reperformed for all following experiments with the BRAFi. PLX is a clinically established inhibitor for the treatment of $BRAF^{V600E}$ mutant melanoma. The inhibitor was applied once 24 h after seeding of the tumor cells. A group of cells were treated with an equivalent amount of DMSO and served as a control. HLA-DR surface expression was analyzed via flow cytometry after 72 h. As shown in *Fig. 1.5*, no substantial decrease of HLA-DR expression could be seen after the treatment.

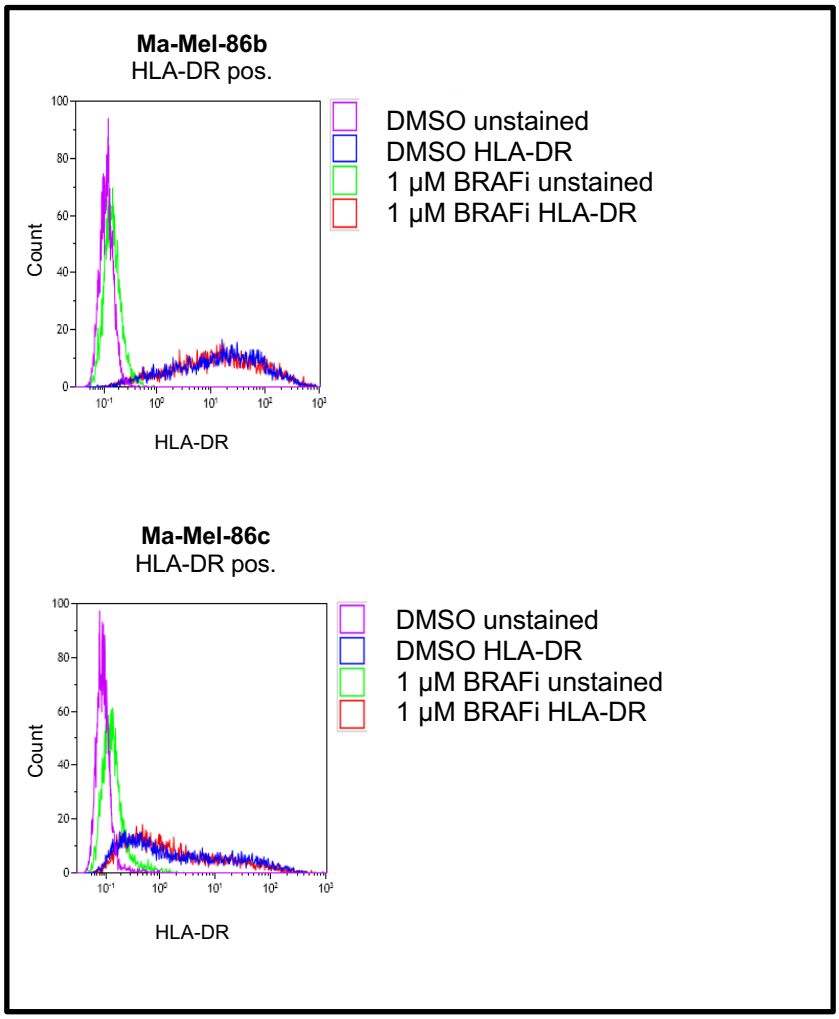

Figure 1.5: 3-day treatment with BRAFi does not lead to a change in HLA-DR surface expression

HLA-DR pos. Ma-Mel-86b and Ma-Mel-86c cells were treated with 1 µM of BRAFi for 72 h or stayed untreated (DMSO) and served as a control before staining of HLA class II surface expression with a PECy7-labelled anti-HLA-DR antibody and analysis via flow cytometry. Representative data from one of three independent experiments shown.

4.3 Effect of AKT pathway inhibition on HLA class II surface expression

Apart from the RAS/RAF/MEK/ERK pathway, the PI3K/AKT pathway is also a key contributor in the development and progression of melanoma and its activation presumably coincides with RAS/RAF/MEK/ERK pathway activation. HLA-DR pos. melanoma cells from Ma-Mel-86b and Ma-Mel-86c were incubated with 2 µM AKT-Inhibitor (AKTi) [GSK2110183 - Afuresertib] for 72 h. GSK2110183 is a pan-AKT inhibitor that binds AKT and inhibits its kinase activity but not its phosphorylation. The inhibitor was applied once 24 h after seeding of tumor cells. A control group of cells was again treated with an equivalent amount of DMSO. This procedure was reperformed for all following experiments with the AKT pathway inhibitor. The effect on the surface expression on HLA-DR was very similar to what had previously been seen with the BRAFi. Again there was no substantial effect on HLA-DR surface expression (*Fig. 1.6*).

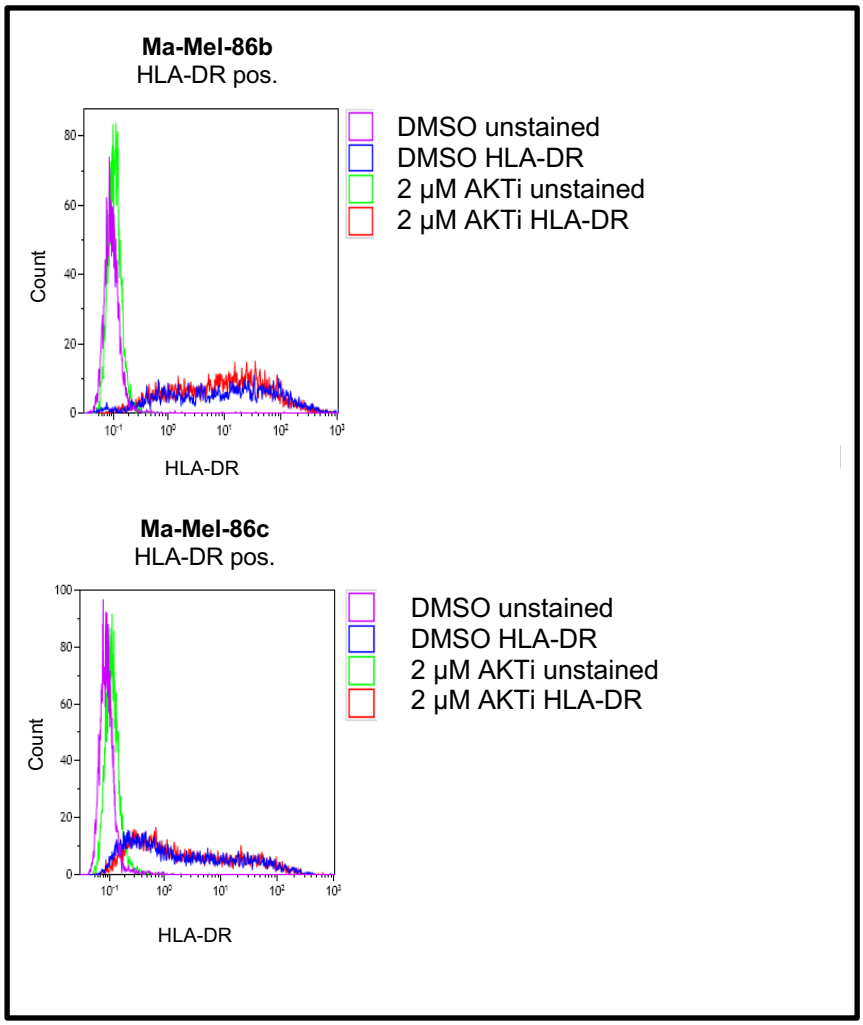

Figure 1.6: 3- day treatment with AKTi does not lead to a change in HLA-DR surface expression

HLA-DR pos. Ma-Mel-86b and Ma-Mel-86c cells were treated with 2 µM of AKTi for 72 h or stayed untreated (DMSO) and served as a control before staining of HLA class II surface expression with a PECy7-labelled anti-HLA-DR antibody and analysis via flow cytometry. Representative data from one of three independent experiments shown.

4.4 Combined treatment with AKT and BRAF inhibitors

Combined treatment with both inhibitors was performed to investigate whether this would impact on HLA class II surface expression, since both pathways are linked to each other and only inhibiting one of the pathways as performed in previous experiments might still have left the cells with enough mechanisms of evading an inhibitory effect on HLA class II. Therefore, Ma-Mel-86b and Ma-Mel-86c cells were treated once with both the AKT- and BRAF- inhibitor (2 µM GSK2110183, 1 µM PLX-4032) for 72 h, 24 h after seeding. When observing the melanoma cells under the microscope, the cells that had undergone the double inhibitor treatment looked different. There were less cells in the incubation flask and the outer appearance seemed less round but instead oval and slender, indicating that treatment did effect the cells. However, the flow cytometry results again showed that also when inhibiting both pathways for 72 h there was no significant effect on the cell's surface expression of HLA-DR proteins.

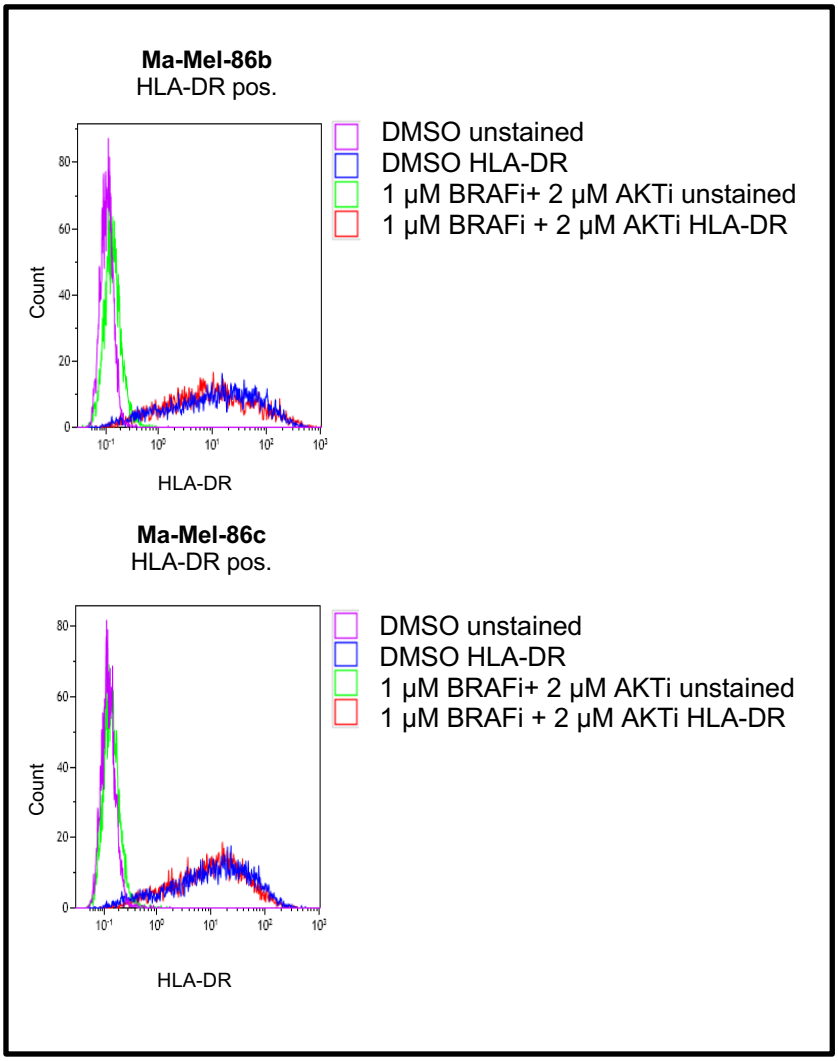

Figure 1.7: 3-day treatment with combined AKTi and BRAFi does not lead to a change in HLA-DR surface expression

HLA-DR pos. Ma-Mel-86b and Ma-Mel-86c cells were treated with 2 µM of AKTi and 1 µM of BRAFi for 72 h or stayed untreated (DMSO) and served as a control before staining of HLA class II surface expression with a PECy7-labelled anti-HLA-DR antibody and analysis via flow cytometry. Representative data from one of three independent experiments shown.

This raised the question whether or not the treatment would show any effect on the endogenous HLA-DR protein levels as well as the levels of key components of both pathways and MDA levels. To study this, Ma-Mel-86b and Ma-Mel-86c were again treated with either the AKTi (2 µM GSK2110183), the BRAFi (1 µM PLX-4032) or a combination of both inhibitors (2 µM GSK2110183 + 1 µM PLX-4032) according to the previous experiments and analyzed via Western Blot (*Fig. 1.8*).

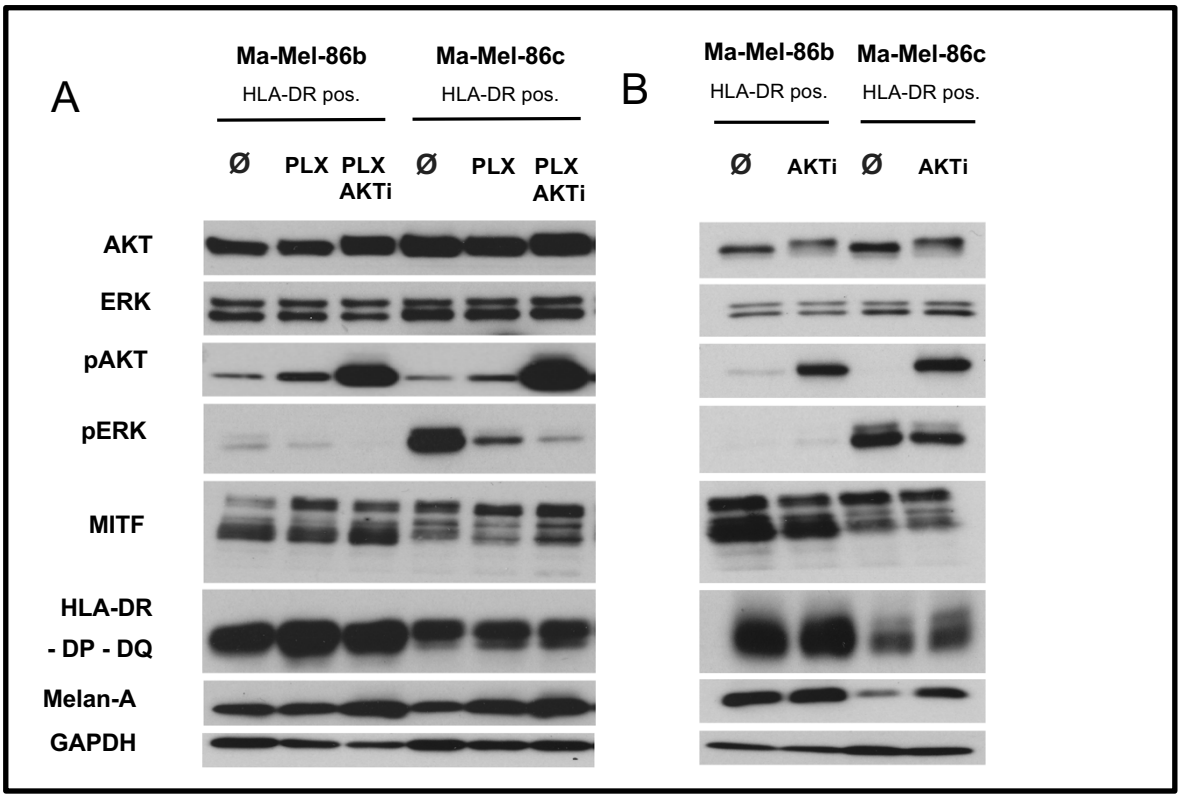

Figure 1.8: BRAFi and combined treatment affects expression of HLA class II molecules and differentiation markers

Cell lysates were analyzed by Western Blot for the protein levels of MAPK and PI3K/AKT pathway components (ERK, AKT, pERK, pAKT), expression of MDA Melan-A and its transcriptional regulator MITF as well as HLA-DR, -DP, -DQ in treated and non-treated Ma-Mel-86b and Ma-Mel-86c.

A) Exemplary Western Blot of DMSO (control Ø), 1 µM BRAFi (PLX) and 1 µM PLX + 2 µM Akt-Inhibitor (PLX+AKTi) treatment for 72 h. GAPDH served as a loading control. Data from one representative of four independent experiments are presented.

B) Western Blot of DMSO (control Ø) and 2 µM AKT-inhibitor (AKTi) treatment for 72 h. Data from one representative of three independent experiments is presented.

GSK2110183 is a pan-AKT inhibitor, decreasing the activity of AKT and its downstream effector targets. Since pAKT expression is normally regulated via negative feedback mechanisms, the loss of AKT activity leads to higher levels of phosphorylated AKT explaining the observed higher signal intensity of pAKT levels in cells treated with the AKTi (*Fig. 1.8 A, Fig. 1.8 B*). As pERK was expressed a lot stronger in Ma-Mel-86c than Ma-Mel-86b the effect of the BRAFi could be seen a lot clearer in this cell line throughout the experiments with a significant loss of pERK expression. It was also interesting to see that the inhibition solely with the BRAFi led to an increased expression of AKT and pAKT in both cell lines indicating that once the MAPK pathway was inhibited the cells leaned more heavily on the PI3K/AKT pathway. Same could not be observed for the single treatment with the AKTi which showed highly alternating to no effects on the expression levels of pERK throughout the experiments.

Furthermore the treatment with the inhibitors seemed to induce an increase in Melan-A expression levels in both cell lines, leading to the presumption that treating melanoma cells with the BRAFi and BRAFi/AKTi might regain certain levels of differentiation within the melanoma cells. In terms of Melan-A expression, the combined treatment with both inhibitors showed the strongest effect on the cells' expression levels, in the form of upregulation, compared to either single treatment alone. These findings suggest a possible synergistic effect when treating cells with a combination of BRAFi/AKTi. Single treatment with the BRAFi led to higher MITF protein expression in both cell lines especially in Ma-Mel-86b. This was not observed with the AKTi where neither Ma-Mel-86b nor Ma-Mel-86c showed strong changes in MITF expression following single treatment.

Looking at MHC-II protein expression levels (HLA-DR, -DP, -DQ), especially Ma-Mel-86b showed an increase following BRAFi and combined treatment contrary to the signal intensity on the surface of the cells where no significant change was observed (*Fig. 1.7*). Ma-Mel-86c also showed the tendency of higher MHC-II protein expression following treatment, however the effect was not as distinct and consistent as with Ma-Mel-86b and showed rather strong alterations especially following combined inhibitor treatment.

The afore mentioned observations were shown more pronounced once the protein expression was quantified by relating the intensity of every protein band to its loading control with ImageJ, a software used for quantification of visual results (*Fig.*

1.9). Since the most significant effects were seen when treating cells with the BRAFi alone or a combination of both inhibitors, focus was put upon these treatments.
In a first step, the signal intensity of each protein band (e.g. HLA-DR) was quantified with ImageJ software, including the band signal intensities of the GAPDH loading controls. This resulted in a numerical value, with a higher value representing a more intense protein band signal. In a second step the acquired numerical values for the protein bands of the treated cells were related to the intensity of their own loading control (e.g. Ma-Mel 86c $\underline{\text{HLA-DR}_{\text{BRAFi}}}$ / Ma-Mel 86c $\underline{\text{GAPDH}_{\text{BRAFi}}}$). For each analyzed protein, the ratio of the DMSO-treated signal intensity (e.g. Ma-Mel 86c $\underline{\text{HLA-DR}_{\text{DMSO}}}$) and the respective GAPDH control signal intensity (Ma-Mel 86c $\underline{\text{GAPDH}_{\text{DMSO}}}$) served as a reference value. Finally, the calculated value of step two was related to the respective reference values of each protein:
$((\text{HLA-DR}_{\text{BRAFi}} / \text{GAPDH}_{\text{BRAFi}}) : (\text{HLA-DR}_{\text{DMSO}} / \text{GAPDH}_{\text{DMSO}}))$.
Relating the intensity of the protein bands to their GAPDH loading control and then normalizing each band to the non-treated (DMSO) GAPDH control was used to decrease the effect of uneven loading of the gel. However, besides the effects of possible uneven loading of the matrigel, it must be noted that the treatment itself may also have led to a decreased expression of GAPDH. Protein band signal intensity for GAPDH was decreased throughout all experiments (*Fig. 1.8, 1.9*). Furthermore, especially the cells that had been treated with a combination of both the AKTi and BRAFi did show severe signs of stress (less cells, oval and slender form) when observed under the microscope. Interestingly, cells treated solely with the AKTi did not show these characteristics. The decrease in GAPDH expression was also observed when analyzing mRNA expression levels of GAPDH in the cells treated with the BRAFi as well as the cells treated with both inhibitors. The cells that had undergone treatment needed significantly more amplification cycles in order to achieve a detectable GAPDH signal than the cells of the control group. Subsequently it was not possible to analyze the data of these cells in the following qPCR experiments.

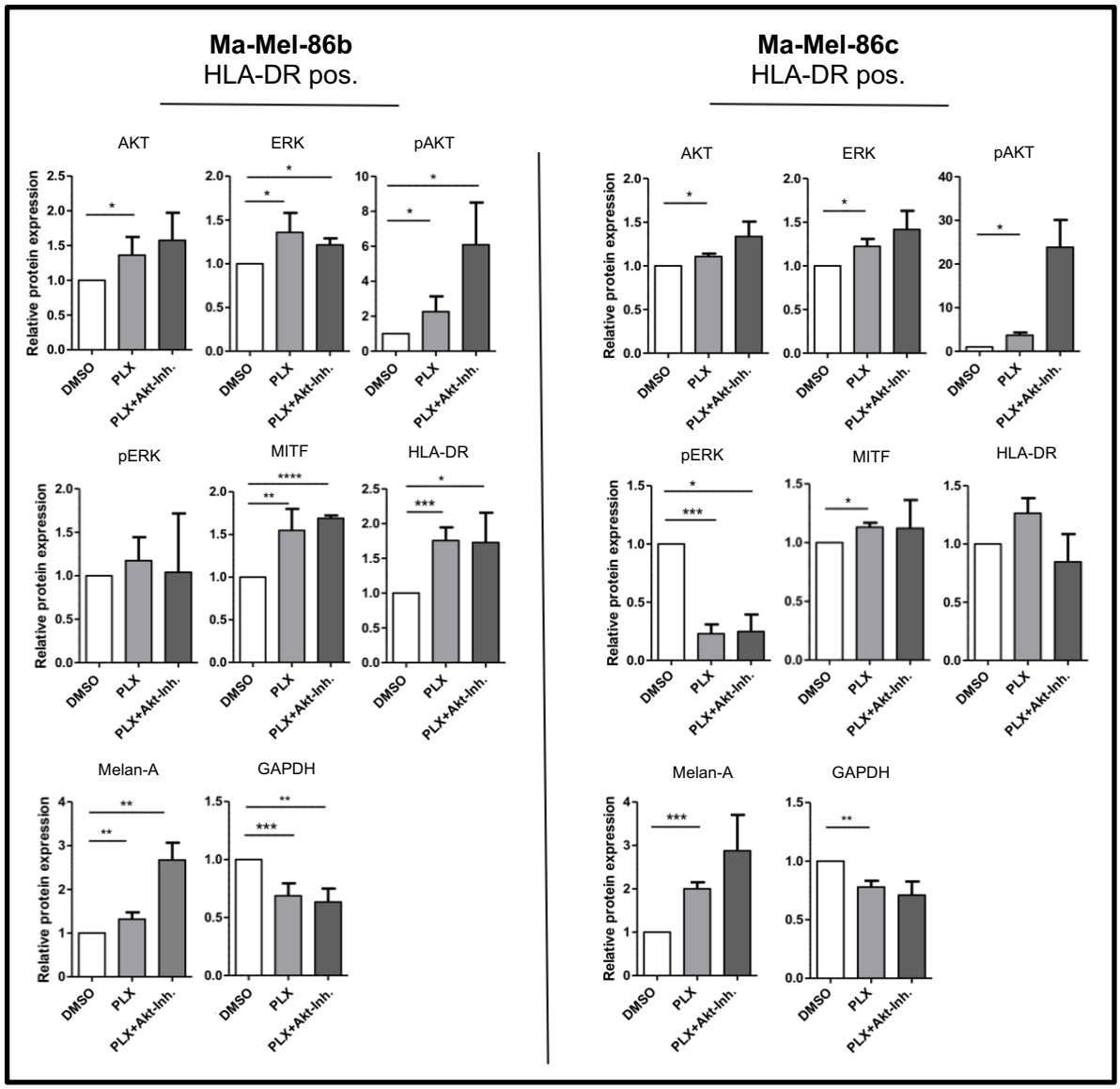

Figure 1.9: Quantification of protein expression after BRAFi and combined treatment

The cells were treated with both the AKTi and the BRAFi (PLX) for 72 h. Protein expression was quantified by relating the intensity of every protein band to its GAPDH loading control (with the exclusion of GAPDH itself) and then normalizing the intensity to the $GAPDH_{DMSO}$ control in order to decrease incorrect measurement caused by unequal loading of the blotting gel. Shown is the mean (+SEM) of at least 3 independent Western Blot quantifications. Statistically significant differences between treated and untreated cells calculated by paired student's t-test is shown; stars/horizontal lines mark samples statistically different from the control (* $p \leq 0.05$, ** $p \leq 0.01$, *** $p \leq 0.005$, **** $p \leq 0.001$).

Therefore, it was only assessed how the AKTi intervened with the mRNA expression levels of the endogenous MHC-II pathway (*Fig. 1.10*). The focus was again put upon *HLA-DRA*, its master regulator *CIITA* as well as its invariant chain *CD74*.

Concomitantly to the tendency of higher protein expression levels of MHC-II (HLA-DR, -DP, -DQ) observed in the Western Blots following treatment (albeit this was seen more pronounced following BRAFi and combined treatment rather than single AKTi treatment), mRNA levels of *HLA-DRA* as well as *CIITA* and *CD74* were significantly higher following AKTi treatment. Again this was especially pronounced and consistent with Ma-Mel-86b, with *CIITA* levels showing a two-fold increase throughout all experiments when compared to untreated cells. However, also Ma-Mel-86c showed the clear tendency of mRNA upregulation of all observed mRNA levels following treatment.

Interestingly, endogenous levels of HLA-DR and its regulator proteins seemed to respond to the treatment with an increase in expression without this leading to an actual gain of HLA-DR on the surface of the cells where it is ultimately found in its antigen presenting function.

In conclusion, the performed treatments, especially with inclusion of a BRAFi did not show any forms of downregulation on MHC-II protein expression. Rather it led to a moderate upregulation in the performed experiments.

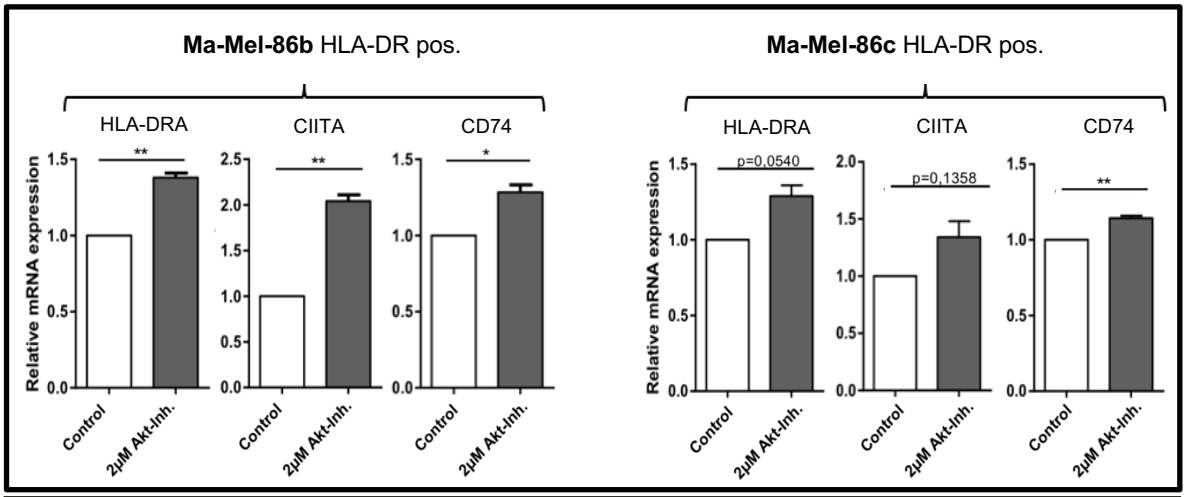

Figure 1.10: Inhibition of AKT pathway leads to higher mRNA levels of *HLA-DRA*, *CIITA* and *CD74*

mRNA levels of *HLA-DRA*, *CIITA* , *CD74* in Ma-Mel-86b and Ma-Mel-86c HLA-DR pos. cells increased after treatment with 2 µM AKTi for 72 h. The treated cells were quantified by qPCR and normalized to endogenous GAPDH mRNA. The relative mRNA amount in the control group was set to 1. Unfortunately there were strong variations in GAPDH levels of the BRAFi treated and the combined inhibitor treated cells therefore these cells could not be analyzed.

Expression levels given as mean (+ SEM) of three independent experiments. Statistically significant differences between treated and untreated cells calculated by paired student's t-test is shown; stars/horizontal lines mark samples statistically different from the control (* $p \leq 0.05$, ** $p \leq 0.01$).

4.5 HLA-DR positive melanoma cells show increased invasiveness

MA-Mel-86c HLA-DR pos. cells showed lower expression levels of MITF. The downregulation of MITF in Ma-Mel-86c has been associated with the enhancement of cell invasiveness by other members of the work group (unpublished data). Thus, Ma-Mel-61a HLA-DR pos. and HLA-DR neg. cells were studied for their invasiveness in order to see whether or not they showed a similar tendency. A matrigel-based invasion assay using the xCELLigence system was performed to see if those cells expressing HLA-DR on their surface might show increased invasiveness. Cells invade from the upper chamber which contains starvation medium and matrigel, through the membrane into the lower chamber containing medium with 10% FBS. Hereby electrical impedance across interdigitated microelectrodes is measured. Increased impedance, automatically recorded by the RTCA instrument, correlates to an increased number of invaded cells.

HLA-DR pos. Ma-Mel-61a as well as the HLA-DR neg. group of Ma-Mel-61a were incubated over a period of 96 h during which their invasiveness was measured (*Fig. 1.11*). Throughout all experiments the graphs showed increased slope values for the HLA-DR pos. cells (green curve) compared to the HLA-DR depleted cells (red curve), indicating increased invasiveness.

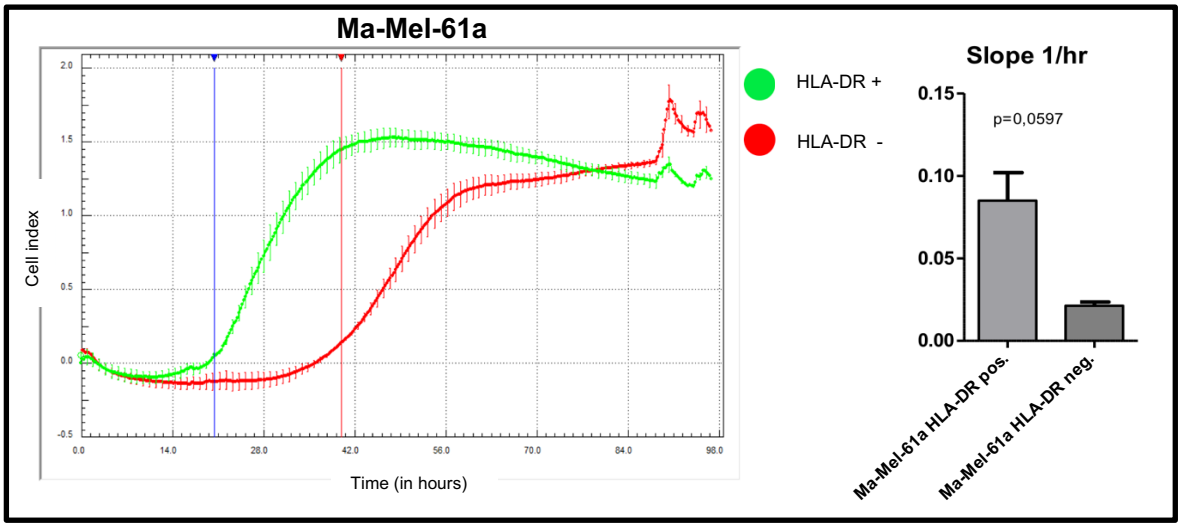

Figure 1.11: Ma-Mel 61a HLA-DR pos. cells show higher invasiveness

Left: 1x10^5 cells/well with a total of 4 wells per cell line were seeded. Cell migration process through microporous gel layer towards chemoattractant (10% FBS medium) was measured every 15 min for a total of 96 h. Cells were cultivated with 2% FBS medium leading up to the experiment for stimulation purposes. Right: The mean (+SEM) of three experiments is shown. Statistically significant differences calculated by paired student's t-test (* $p \leq 0.05$).

5 DISCUSSION

5.1 The relevance of MHC-II expression in melanoma

For many years it has been known that some melanoma cells show constitutive MHC-II surface expression on their cell surface. Until today it is not entirely understood why melanoma cells do this and to which extent it affects the progression of the disease.

In 1984 Bröcker et. al hypothesized that the level of MHC-II expression was related to the level of invasiveness, the density of intratumoral mononuclear cell infiltrate, the incidence of early metastases and the tumor thickness. Their study found that a high expression of MHC-II was associated to a non-favorable prognosis in patients with primary melanoma (Brocker et al., 1984).

Aoudjit et al. followed the hypothesis of MHC-II expression being related to a worse patient outcome by claiming that in melanoma cells expressing MHC-II proteins on their surface the HLA-DR signaling following T-cell recognition via Lymphocyte-Activation-Gene-3 (LAG-3), a ligand often expressed on tumor cell infiltrating lymphocytes, led to an activation of the MAPK/ERK pathway which in conclusion had a functional role in the melanoma cells' resistance to FAS mediated apoptosis (Aoudjit et al., 2004). Like Aoudjit et al., Hemon et al. concluded that *in vitro* the interaction of MHC-II on tumor cells with the LAG-3 ligand on T-cells led to an upregulation of the MAPK/ERK and PI3K/AKT pathways in melanoma cells negatively regulating T-cell proliferation, function, and homeostasis (Hemon et al., 2011). Of particular interest in Johnson et al.'s 2018 analysis of tumor cell's protein surface expression patterns was the association of HLA-DR tumor cell positivity with LAG3, which actively competes with CD4 as a ligand for MHC-II, leading to a suppression of MHC-II–mediated antigen presentation (Johnson et al., 2018).

Another interesting *in vitro* observation is that tumor specific CD4+ T-cells attracted to the tumor environment by MHC-II bearing tumor cells dominantly express TNFα which might dampen CD8+ T-cell anti-tumor response by counteracting and reducing the IFN-γ-mediated immune responses of CD8+ T-cells. This would present an immune escape mechanism for those tumor cells expressing MHC-II (Donia et al., 2015).

So far the most widely recognized function of MHC-II molecules is the presentation of antigens to T-lymphocytes. However, engagement of these molecules, e.g. by specific antibodies, could also lead to the activation of specific signaling pathways in melanoma cells. Barbieri et al. postulated that signals mediated via the engagement of MHC-II on melanoma cells may influence antigen-presenting function, frustrating an active anti-tumor response (Barbieri et al., 2011).

Of note, in a very recent study from 2017 Costantini reported that MHC-II mediated signaling increases melanoma cell migration and invasion in vitro (Costantini et al., 2017). As shown in *Fig. 1.12* of this study the subpopulation of HLA-DR pos. Ma-Mel-61a cells sorted from their bulk cell line indeed showed a higher level of invasiveness, supporting a possible connection between HLA-DR expression and higher invasiveness.

Our research group further showed that HLA-DR pos. cells show an upregulation of markers known from Epithelial-Mesenchymal Transition (EMT) such as Fibronectin (Heeke et al., unpublished). These markers imply a dedifferentiation process in melanoma cells referred to as an “EMT-like phenotypic switch” since melanocytes, from which melanoma derives, are not epithelial cells. EMT in general is a biologic process where initially polarized epithelial cells lose their apical-basal polarity and undergo biochemical changes, including alterations to the cytoskeleton and cell shape, that lead to a mesenchymal cell phenotype. These changes, among others, increase migratory capacity and enable the development of an invasive phenotype (Kalluri & Weinberg, 2009). Whether or not HLA-DR expression and EMT are intertwined has to be further investigated.

To solidify this assumption further experiments with other HLA-DR pos. cell lines would be necessary. Furthermore this study solely focused on the different invasion behavior of non-treated HLA-DR pos. and neg. cells. It would be interesting to examine whether or not melanoma cells treated with PLX-4032 or AKT pathway inhibitor GSK2110183 show less invasive behavior in an xCELLigence invasion assay.

In contrast, other recent studies also indicate the contrary and state that MHC-II expression on cancer cells might even be associated with a longer patient survival. Anichini et al. compared the overall survival of stage III and IV melanoma patients and concluded that a higher expression of MHC-II molecules was associated with a significantly longer overall survival, measured as time from surgical removal of the

metastatic lesion to death (Anichini et al., 2006). They stated that T-cell–mediated antitumor response may possibly be more effective (at either the priming and/or effector phases) in metastatic lesions with retained or higher levels of expression of MHC-II antigens. This correlated with findings in other types of cancer expressing MHC-II such as the colorectal cancer (Matsushita et al., 2006). Although Matsushita himself describes higher concentration of IFN-γ in the adjacent tissue as the possible main immunological mechanism involved in the better long-term survival of colorectal cancer patients and higher MHC-II expression.

Chen et al. analyzed microarray and RNA-Sequence data of cutaneous melanoma cells constitutively expressing MHC-II from *The Cancer Genome Atlas* and investigated a total of 480 clinical samples and correlated the expression pattern to overall patient survival. Their survival analysis showed longer survival in patients with higher MHC-II expression as compared to those with low/medium expression and also the tendency of an increase in expression from stage II to stage IV melanoma patients. Especially higher expression of the subtypes *HLA-DR* and *-DP* was associated to longer patient survival. In other cancer types expressing MHC-II such as sarcoma, lung adenocarcinoma and invasive breast carcinoma higher expression showed similar findings, however the highest correlation was found in melanoma. Expression was observed to be different between tissue samples and *in vitro* melanoma cells, leading to the assumption that tumor microenvironment plays a significant role in MHC-II expression as well as its antigen presentation function. Interestingly Chen et al. found the co-expression of *CD74* (aside from 10 other genes) to be the most closely conjugated gene in terms of biological functions related to antigen processing and presentation and immune response (Chen et al., 2019).

In summary, it is conceivable that MHC-II expression on cancer cells in general has both positive and negative effects on the patient's overall survival depending on the stage of tumor progression, entity, the tumor's microenvironment as well as the subtype of the primary melanoma lesion.

5.2 HLA-DR positive cells show higher protein levels of pERK

Another interesting aspect to the studied melanoma cells expressing HLA-DR molecules on their cell surface are the higher levels of pERK that could be found throughout all tested cell lines, especially Ma-Mel-86c and Ma-Mel-61a, suggesting an association between the MAPK pathway and HLA-DR expression.

When treating the cells Ma-Mel-86b and Ma-Mel-86c with PLX-4032 (Vemurafenib) the most proven $BRAF^{V600E}$-specific MAPK pathway inhibitor, Western Blots showed that especially Ma-Mel-86c, as expected, reacted in a significant loss of pERK expression (*Fig. 1.8; 1.9*). However, none of the cells showed a decrease in HLA-DR expression neither on the surface of the cells nor at the total protein level (*Fig. 1.5; 1.8; 1.9)*. On the contrary both Ma-Mel-86b and Ma-Mel-86c rather showed equivalent or moderately upregulated HLA-DR protein expression following the treatment, this suggests that either the treatment time of 72 h might not have been long enough or the applied inhibitor of the MAPK pathway simply did not have an effect on the HLA-DR expression of our melanoma cell lines. Also adding the AKT-inhibitor GSK2110183 to the PLX-4032 treatment and thus blocking two pathways did not lead to a detectable downregulation of HLA-DR protein- or surface expression under the selected experimental conditions (*Fig. 1.7-1.9*). AKTi treatment alone showed consistently higher mRNA levels of *HLA-DRA*, *CD74* and *CIITA* (*Fig. 1.10*), without any change on MHC-II surface expression (*Fig. 1.6*) and at least our experiments did not show a reactive upregulation of pERK on a protein level (*Fig. 1.8 B*). A possible explanation could be that the analyzed cell lines lean more heavily on the MAPK/ERK pathway for proliferation which would explain why solely inhibiting the PI3K/AKT pathway showed little effect on the proteins of the MAPK/ERK pathway. However, inhibiting the PI3K/AKT pathway might have stimulated non-analyzed pathways associated with MHC-II expression, explaining the upregulation of *HLA-DRA, CIITA* and *CD74*.

So far there is no research upon the half-lives of MHC-II molecules expressed in melanoma cells, however looking at APCs, e.g. dendritic cells, half-lives ranging from 10 h in immature dendritic cells up to 100 h in mature dendritic cells have been documented depending on inflammatory signals in the cells' microenvironment (Cella et al., 1997). Assuming that MHC-II molecules in melanoma cells have similar half-lives as compared to APCs our treatment duration of 72 h might indeed not

have been long enough to actually show a significant loss of MHC-II concentration, be it on the protein level or on the surface of the cells, where MHC-II levels might have been to saturated in order to actually detect alterations in expression. Increasing the treatment duration or even the concentration of the BRAFi and AKTi was however too much stress for the melanoma cells *in vitro* which is why we chose to go on with the same treatment procedure.

All in all these findings indicate that there may be other pathways at play regulating MHC-II expression which were not considered or that the pathways were not affected to a degree where MHC-II expression was actually limited.

Non the less, recent studies show that the MAPK/ERK pathway indeed seems to play a significant role in melanoma cells constitutively expressing MHC-II by identifying a MAPK-responsive enhancer motif (AP-1), 6 kb upstream from pIII (promoter III) which regulates *CIITA* expression (Martins et al., 2007). Martins et al. saw a downregulation of MHC-II and *CIITA* expression in both FACS and qPCR following MAPK pathway inhibition. Instead of PLX-4032, Martins et al. applied different MAPK-ERK and -JNK (NH2-terminal kinase, another major group of MAPK in mammalian cells besides ERK) inhibitors. The A375 melanoma cell line used in their study was treated for 24 h with various inhibitors, as opposed to the 72 h treatment with PLX-4032 of this study. The most significant decrease of MHC-II cell surface expression was observed after treatment with U0126, a MAPK-ERK kinase (Mek1)-specific inhibitor, still in preclinical trials. Other (Mek1)-specific inhibitors such as Trametinib and Cobimetinib however have been approved by the US Foods and Drug Administration (FDA) for treatment of melanoma (Cheng et al., 2017). It is possible, that while there was a significant decrease in pERK expression following PLX-4032 treatment throughout the experiments of this study the remaining levels of pERK may still have been high enough to affect the cells' HLA-DR expression. Even if our results did not show similar effects on the melanoma cells there are promising developments in the field of MAPK-ERK kinase specific inhibitors and it should be further investigated as to how different inhibitors and treatment durations affect HLA-DR protein levels. To which extent that might benefit future therapy options for affected patients remains the focus of further studies.

Also, the different characteristics of melanoma cell subpopulations resulting from de-differentiation processes cannot be understated when observing the effects of treatment with specific pathway inhibitors. Certainly many more melanoma

subpopulations must be analyzed in order to receive a better understanding of the diverse pathways at play in order to make more educated assumptions on treatment effects.

5.3 BRAFi and combined treatment with AKTi leads to an upregulation of Melan-A in HLA-DR positive cells

Along with the MAPK/ERK pathway the PI3K/AKT pathway plays a significant role in melanoma initiation, development and de-differentiation processes (Dantonio et al., 2018). In this study, sorted HLA-DR pos. melanoma cells were treated with GSK2110183 (Afuresertib), an AKT-inhibitor which was tested in a phase 2 clinical trial completed in June of 2018 (*https://clinicaltrials.gov/ct2/show/NCT01531894*).
Especially when combining the AKTi with PLX-4032, our experiments showed an upregulation of Melan-A and also MITF protein expression superior to that of either inhibitor alone (*Fig. 1.8; 1.9*). The effects were similar for both Ma-Mel-86b (lower expression levels of pERK and higher levels of Melan-A) and Ma-Mel-86c (high expression levels of pERK and low expression levels of Melan-A). These findings correlated with those of Donia et al. in 2012 who had also observed an upregulation of MDAs (incl. Melan-A) following treatment of melanoma cells with Vemurafenib. It would have been interesting to see what the increased protein expression led to on an mRNA level, however the *in vitro* treatment itself proved very stressful for the cultivated cells (less cells, slender form) leading to strong variations in the reference genes GAPDH and also when ß-Actin was used as a reference which made qPCR analyzation impossible. Further experiments investigating the effect of the treatment on an mRNA level are therefore necessary, possibly using a lower concentration of the inhibitors, shorter treatment duration or other reference genes. It also remains to be analyzed whether or not the observed elevated endogenous levels of Melan-A lead to a higher expression on the cell surface as this was not the case with MHC-II in our experiments.
Downregulation of MDAs, e.g. Melan-A in melanoma, is an escape mechanism observed in tumor cells to evade recognition by the immune system. If a combined treatment leads to an upregulation of MDAs it may prove to be essential in future therapy programs by achieving to demask melanoma cells that had previously

evaded immune surveillance. Since this study only regarded Melan-A expression further experiments looking at the expression levels of other MDAs (e.g. gp100 and Tyrosinase) are necessary.

Furthermore only HLA-DR sorted cell lines were assessed in our experiments. Treating bulk cell lines with PLX seemingly showed similar effects on Melan-A and MITF expression (*Supplementary Figure 1A*), however further experiments are necessary to solidify this observation.

Another important aspect to consider in terms of tumor immunogenicity is the question whether or not the observed upregulation of MDAs following anti-tumor-treatment is transient or permanent, regarding the fact that for instance clinical response to BRAFi treatment is often limited due to cells developing resistance mechanisms to treatment over time. Following up on that question our work group treated Ma-Mel-86c (and Ma-Mel-63) cells with BRAFi (Vemurafenib) and a combination of BRAFi/MEKi (Vemurafenib + Trametinib) which is replacing BRAFi monotherapy as the standard of care treatment for $BRAF^{V600}$ mutant melanomas. Cells were treated over different time periods ranging from 3 – 21 d and afterwards incubated with autologous CD8+ tumor-infiltrating lymphocytes. TILs recognition was measured by analyzing TNFα and IFN-γ expression levels by the CD8+ lymphocytes. Interestingly, TNFα and IFN-γ levels were highest after a treatment duration of 3 – 7 d and decreased with increasing treatment duration. The lack of tumor cell recognition by the TILs following longer treatment was linked to strong alterations of the tumor antigen expression profile over time (including downregulation of Melan-A), resulting in resistance against CD8+ T-cells. This was true for both mono- and combined therapy. Pairing kinase-targeted therapy with immunotherapy early on in treatment protocols therefore seems like a promising aspect in preventing the development of immune-evasive tumor variants (Pieper et al., 2018). The aim to maintain an immunogenic environment with high levels of MDA expression, at best permanently, cannot be understated with the importance of highly specific, patient oriented CD4+ ACT playing an increasingly larger role in driving anti-tumor immunity and in supporting anti-tumor CD8+ T-cell responses with observations that a higher CD4/CD8 ratio used to generate CAR T-cells correlated with better clinical response in certain cancer types (Tay et al., 2020).

5.4 Detection of HLA-DR expression for future immunotherapies

All melanoma cell lines analyzed in this study showed subpopulations of cells constitutively expressing HLA-DR on their cell surface (*Fig. 1.1*).

Johnson et al. found that melanoma cells expressing HLA-DR on their cell surface (either constitutively or heterogeneously) concomitantly express PD-L1 to a higher degree and showed significantly better response to Anti-PD-1 therapy. HLA-DR could therefore be of interest as a biomarker for therapeutic efficacy (Johnson et al., 2016). The reason for the correlation between HLA-DR and PD-L1 expression is not entirely clear, an interesting hypothesis is that MHC-II expression on melanoma cells could be an immune-evasive effort to attract regulatory T-cells (T-reg.) a subtype of T-cells drawn to inflammatory sites in an effort to suppress overreactions by the adaptive immune system. T-reg. differentiation and interaction is a process that requires PD-L1 expression by the tumor cells; therefore interruption of this signaling could indeed be beneficial in MHC-II pos. tumors.

Recently Rodig et al. followed up on Johnson et al. stating that primary response and better outcome to Anti-PD-1 therapy was associated to pre-existing MHC-II tumor expression especially when MHC-I was compromised. The better outcome in MHC-II pos. melanoma patients was also associated to a more immunogenic environment (IFN-γ being the strongest inducer of MHC-II expression) (Rodig et al., 2018).

Approximately 60% of patients show primary (de-novo) resistance to PD-1 checkpoint inhibition and 20−30% of initial responders will develop secondary (acquired) resistance (Schadendorf et al., 2018). Johnson et al. followed up on their studies from 2016 and showed that one mechanism of acquired resistance to PD-1 therapy occurring in MHC-II pos. tumors could be the upregulation of inhibitory MHC-II ligands, (i.e. LAG-3 as mentioned above) during disease progression. MHC-II positivity on tumor cells thus provides selective pressure for LAG-3 positive TILs to suppress MHC-II–mediated antigen presentation leading to lesser antitumor immunity. Another promising immunotherapeutic combination for the future could therefore be that of PD-1/PD-L1 and LAG-3 blockade, specific for MHC-II–expressing tumors (Johnson et al., 2018).

In regard to the still high numbers of initial and acquired resistance to Anti-PD-1/PD-L1 therapy it is thereby important to further understand the complex pathways

behind antitumor immunity and to identify those patients susceptible to different approaches of immunotherapy. Recognizing MHC-II expression in melanoma patients seems to be a promising strategy since the current available tests and methods used to identify PD-L1 expression in patient melanoma cells are both expensive and complex, checking for HLA-DR expression on cells is however a lot more affordable by using commercially available antibodies. Further understanding the mechanics behind HLA-DR expression on tumor cells and its correlation to PD-L1 expression in general could prove to be an important selection factor leading to the prevention of unnecessary medical side effects and costs caused by ill-advised drug application.

5.5 Differences between the investigated HLA-DR positive melanoma cell lines

As mentioned above Western Blots showed pERK upregulated in all HLA-DR sorted cell lines, especially in Ma-Mel-86c and Ma-Mel-61a and also, however not as strongly, in Ma-Mel-86b. Especially in the Ma-Mel-86 cell lines, which originate from the same patient, the higher levels of pERK in Ma-Mel-86c indicate that the MAPK pathway seemed to play a significant role in disease progression and tumor proliferation. Inhibition of the MAPK pathway led to an increase in pAKT levels for both Ma-Mel-86b and Ma-Mel-86c showing that inhibition of one pathway leads the de-differentiated cells to quickly upregulate other pathways. Ma-Mel-61a cells were not treated with inhibitors in this study but results in our work group indicate the same behavior following treatment. As written above there are indications to a correlation between the activation of the MAPK pathway and HLA-DR expression. However simply inhibiting the pathway did not lead to a downregulation of HLA-DR neither on a protein expression level nor on the surface of the cells in the performed experiments indicating further mechanisms involved.

Concomitant to noticeably higher pERK levels, MDA Melan-A protein expression was downregulated in HLA-DR pos. subpopulations of Ma-Mel-86c and Ma-Mel-61a. An indicator of advanced de-differentiation in these two cell lines. Besides the many afore mentioned theories in terms of MHC-II expression in melanoma, it is conceivable that HLA-DR expression might simply be a surrogate parameter of de-differentiation in melanoma cells, possibly due to the loss of so far unknown

regulating pathways during de-differentiation. Interestingly however, Ma-Mel-86b did not show the same Melan-A downregulation and pERK upregulation in HLA-DR sorted cells compared to its bulk cell line in our Western Blots, possibly due to the fact, that this cell line was from an earlier metastasis compared to the other cell lines. These discrepancies show that it is essential that more constitutively MHC-II expressing subpopulations of melanoma cells are examined especially in terms of MDA expression patterns in order to further understand the mechanisms behind this occurrence.

6 SUMMARY

Melanoma remains the most common cause of death among patients with skin cancer. The most common oncogenic $BRAF^{V600E}$ mutation induces a constitutive activation of the mitogen-activated protein kinase (MAPK) signaling pathway. Likewise mutations affecting the phosphoinositide 3-kinase (PI3K) / Protein kinase B (AKT) pathway have been found in more advanced melanoma. Therapy resistance to pathway inhibitors and immunotherapy remains a major challenge in the treatment of metastatic patients. Improvement of therapy outcome depends on studies linking melanoma cell biology and immunology. Interestingly, a subset of melanoma cells constitutively expresses Human Leukocyte Antigen class II (HLA-II) surface molecules presenting antigens to CD4+ T-cells. Physiologically, HLA-II expression is restricted to professional antigen presenting cells and so far the regulation of constitutive HLA-II expression in melanoma is poorly defined. This project studied MAPK and PI3K/AKT signaling in the regulation of HLA-II expression, linking HLA-II positivity to tumor cell differentiation. HLA-II expressing melanoma subpopulations were separated from three bulk cell lines (Malignant-Melanoma (Ma-Mel) -61a, -86b, -86c). Western blot analyses revealed lower expression of differentiation proteins in two HLA-II positive (pos.) melanoma populations and all three HLA-II pos. cell subsets showed higher levels of pERK, suggesting HLA-II expression could be linked to the MAPK pathway. 72 hour treatment of these cells with a specific $BRAF^{V600E}$ inhibitor however did not affect HLA-II surface expression. Similar results were obtained when treating with combined inhibitors targeting the PI3K/AKT and MAPK pathways. Protein analyses showed a slight increase in total HLA-II expression, as well as differentiation proteins (Melan-A) after combined inhibitor treatment in two cell lines. According to the more de-differentiated cell state, HLA-II pos. melanoma cells showed higher invasiveness (Ma-Mel-61a). In summary, this study demonstrated elevated activation of the MAPK pathway in HLA-II pos. melanoma cells but blocking the pathway did not affect HLA-DR surface expression. These findings suggest that under the experimental conditions tested, MAPK signalling is not driving constitutive HLA class II expression indicating involvement of other mechanisms.

Zusammenfassung

Das Melanom ist nach wie vor die häufigste Todesursache bei Patienten mit Hautkrebs. Die häufigste onkogene $BRAF^{V600E}$-Mutation induziert eine konstitutive Aktivierung des mitogen-activated protein kinase (MAPK)-Signalweges. Mutationen, die den Phosphoinositid-3-Kinase (PI3K) / Proteinkinase B (AKT)-Signalweg betreffen, wurden bei fortgeschrittenen Melanomen gefunden. Die Therapieresistenz stellt nach wie vor die größte Herausforderung bei der Behandlung des metastasierten Melanoms dar. Die Verbesserung der Therapieergebnisse hängt von Studien ab, die die Biologie der Melanomzellen und die Immunologie miteinander verbinden. Interessanterweise exprimieren eine Untergruppe von Melanomzellen konstitutiv Humanes Leukozyten-Antigen Klasse II (HLA-II) auf ihrer Oberfläche, worüber sie CD4+ T-Zellen Antigene präsentieren. Physiologisch ist die HLA-II Expression auf professionelle Antigen-präsentierende Zellen beschränkt, und die Regulierung der konstitutiven HLA-II-Expression im Melanom bisher nur unzureichend untersucht. Dieses Projekt untersuchte die MAPK- und PI3K/AKT-Signalübertragung bei der Regulierung der HLA-II-Expression und stellte eine Verbindung zwischen der HLA-II-Positivität und der Tumorzelldifferenzierung her. Western-Blot-Analysen ergaben eine geringere Expression von Differenzierungsproteinen in zwei HLA-II-positiven (pos.) Melanompopulationen, und drei HLA-II pos. Zellsubpopulationen wiesen höhere pERK-Werte auf, was darauf hindeutet, dass die HLA-II-Expression mit dem MAPK-Signalweg verbunden sein könnte. Eine 72-stündige Behandlung dieser Zellen mit einem spezifischen BRAFV600E-Inhibitor hatte jedoch keinen Einfluss auf die HLA-II-Oberflächenexpression. Ähnliche Ergebnisse wurden bei einer kombinierten Behandlung mit PI3K/AKT- und MAPK-Signalweg Inhibitoren erreicht. Proteinanalysen zeigten einen leichten Anstieg der gesamten HLA-II-Expression sowie des Differenzierungsproteins Melan-A nach der Behandlung mit kombinierten Inhibitoren in zwei Zelllinien. Dem stärker entdifferenzierten Zellzustand entsprechend zeigten HLA-II-pos. Melanomzellen eine höhere Invasivität. Zusammenfassend zeigte die Blockierung des MAPK-Signalwegs keinen Einfluss auf die HLA-II-Oberflächenexpression. Dies deutet auf die Beteiligung anderer Mechanismen für die konstitutive HLA-Klasse-II-Expression hin.

7 REFERENCES

1. Aguissa-Touré, A.-H., Li, G. (2012). Genetic alterations of PTEN in human melanoma. *Cellular and Molecular Life Sciences*, *69*(9), 1475–1491. https://doi.org/10.1007/s00018-011-0878-0
2. Al-Shibli, K. I., Donnem, T., Al-Saad, S., Persson, M., Bremnes, R. M., Busund, L.-T. (2008). Prognostic effect of epithelial and stromal lymphocyte infiltration in non-small cell lung cancer. *Clinical Cancer Research : An Official Journal of the American Association for Cancer Research*, *14*(16), 5220–5227. https://doi.org/10.1158/1078-0432.CCR-08-0133
3. Anichini, A., Mortarini, R., Nonaka, D., Molla, A., Vegetti, C., Montaldi, E., Wang, X., Ferrone, S. (2006). Association of Antigen-Processing Machinery and HLA Antigen Phenotype of Melanoma Cells with Survival in American Joint Committee on Cancer Stage III and IV Melanoma Patients. *Cancer Research*, *66*(12), 6405–6411. https://doi.org/10.1158/0008-5472.CAN-06-0854
4. Aoudjit, F., Guo, W., Gagnon-Houde, J.-V., Castaigne, J.-G., Alcaide-Loridan, C., Charron, D., Al-Daccak, R. (2004). HLA-DR signaling inhibits Fas-mediated apoptosis in A375 melanoma cells. *Experimental Cell Research*, *299*(1), 79–90. https://doi.org/10.1016/j.yexcr.2004.05.011
5. Atefi, M., von Euw, E., Attar, N., Ng, C., Chu, C., Guo, D., Nazarian, R., Chmielowski, B., Glaspy, J., Comin-Anduix, B., Mischel, P., Lo, R., Ribas, A. (2011). Reversing melanoma cross-resistance to BRAF and MEK inhibitors by co-targeting the AKT/mTOR pathway. *PloS One*, *6*(12), e28973. https://doi.org/10.1371/journal.pone.0028973
6. Barbieri, G., Rimini, E., Costa, M. A. (2011). Effects of human leukocyte antigen (HLA)-DR engagement on melanoma cells. *International Journal of Oncology*, *38*(6), 1589–1595. https://doi.org/10.3892/ijo.2011.988
7. Bernatchez, C., Radvanyi, L. G., Hwu, P. (2012). Advances in the treatment of metastatic melanoma: adoptive T-cell therapy. *Seminars in Oncology*, *39*(2), 215–226. https://doi.org/10.1053/j.seminoncol.2012.01.006
8. Brocker, E.-B. E., Suter, L., Sorg, C. N. (1984). *HLA-DR Antigen Expression in Primary Melanomas of the Skin* (Vol. 82).

9. Burnet, M. (1957). Cancer; a biological approach. I. The processes of control. *British Medical Journal*, *1*(5022), 779–786.
10. Carreira, S., Goodall, J., Denat, L., Rodriguez, M., Nuciforo, P., Hoek, K. S., Testori, A., Larue, L., Goding, C. R. (2006). Mitf regulation of Dia1 controls melanoma proliferation and invasiveness. *Genes & Development*, *20*(24), 3426–3439. https://doi.org/10.1101/gad.406406
11. Cella, M., Engering, A., Pinet, V., Pieters, J., Lanzavecchia, A. (1997). Inflammatory stimuli induce accumulation of MHC class II complexes on dendritic cells. *Nature*, *388*(6644), 782–787. https://doi.org/10.1038/42030
12. Chen, Y.-Y., Chang, W.-A., Lin, E.-S., Chen, Y.-J., Kuo, P.-L. (2019). Expressions of HLA Class II Genes in Cutaneous Melanoma Were Associated with Clinical Outcome: Bioinformatics Approaches and Systematic Analysis of Public Microarray and RNA-Seq Datasets. *Diagnostics (Basel, Switzerland)*, *9*(2). https://doi.org/10.3390/diagnostics9020059
13. Cheng, Y., Tian, H. (2017). Current Development Status of MEK Inhibitors. *Molecules*, *22*(10), 1551. https://doi.org/10.3390/molecules22101551
14. Cheung, M., Sharma, A., Madhunapantula, S. V., Robertson, G. P. (2008). Akt3 and mutant V600E B-Raf cooperate to promote early melanoma development. *Cancer Research*, *68*(9), 3429–3439. https://doi.org/10.1158/0008-5472.CAN-07-5867
15. Costantini, F., Barbieri, G. (2017). The HLA-DR mediated signalling increases the migration and invasion of melanoma cells, the expression and lipid raft recruitment of adhesion receptors, PD-L1 and signal transduction proteins. *Cellular Signalling*, *36*, 189–203. https://doi.org/10.1016/j.cellsig.2017.05.008
16. D'Mello, S. A. N., Finlay, G. J., Baguley, B. C., Askarian-Amiri, M. E. (2016). Signaling Pathways in Melanogenesis. *International Journal of Molecular Sciences*, *17*(7). https://doi.org/10.3390/ijms17071144
17. Dantonio, P. M., Klein, M. O., Freire, M. R. V. B., Araujo, C. N., Chiacetti, A. C., Correa, R. G. (2018). Exploring major signaling cascades in melanomagenesis: a rationale route for targetted skin cancer therapy. *Bioscience Reports*, *38*(5). https://doi.org/10.1042/bsr20180511
18. de Charette, M., Marabelle, A., Houot, R. (2016). Turning tumour cells into

antigen presenting cells: The next step to improve cancer immunotherapy? *European Journal of Cancer*, *68*, 134–147. https://doi.org/10.1016/J.EJCA.2016.09.010

19. Deffrennes, V., Vedrenne, J., Stolzenberg, M. C., Piskurich, J., Barbieri, G., Ting, J. P., Charron, D., Alcaïde-Loridan, C. (2001). Constitutive expression of MHC class II genes in melanoma cell lines results from the transcription of class II transactivator abnormally initiated from its B cell-specific promoter. *Journal of Immunology (Baltimore, Md. : 1950)*, *167*(1), 98–106.
20. Diamantopoulos, P., Gogas, H. (2016). Melanoma immunotherapy dominates the field. *Annals of Translational Medicine*, *4*(14), 269. https://doi.org/10.21037/atm.2016.06.32
21. Donia, M., Andersen, R., Kjeldsen, J. W., Fagone, P., Munir, S., Nicoletti, F., Andersen, M. H., Straten, P. T., Svane, I. M. (2015). Aberrant Expression of MHC Class II in Melanoma Attracts Inflammatory Tumor-Specific CD4 $^{+}$ T-Cells, Which Dampen CD8 $^{+}$ T-cell Antitumor Reactivity. *Cancer Research*, *75*(18), 3747–3759. https://doi.org/10.1158/0008-5472.CAN-14-2956
22. Donia, M., Fagone, P., Nicoletti, F., Andersen, R. S., Høgdall, E., Straten, P. T., Andersen, M. H., Svane, I. M. (2012). BRAF inhibition improves tumor recognition by the immune system: Potential implications for combinatorial therapies against melanoma involving adoptive T-cell transfer. *Oncoimmunology*, *1*(9), 1476–1483. https://doi.org/10.4161/onci.21940
23. Ferradini, L., Mackensen, A., Genevée, C., Bosq, J., Duvillard, P., Avril, M. F., Hercend, T. (1993). Analysis of T cell receptor variability in tumor-infiltrating lymphocytes from a human regressive melanoma. Evidence for in situ T cell clonal expansion. *The Journal of Clinical Investigation*, *91*(3), 1183–1190. https://doi.org/10.1172/JCI116278
24. Flaherty, K. T., Infante, J. R., Daud, A., Gonzalez, R., Kefford, R. F., Sosman, J., Hamid, O., Schuchter, L., Cebon, J., Ibrahim, N., Kudchadkar, R., Burris, H. A., Falchook, G., Algazi, A., Lewis, K., Long, G. V., Puzanov, I., Lebowitz, P., Singh, A., Little, S., Sun, P., Allred, A., Ouellet, D., Kim, K. B., Patel, K., Weber, J. (2012). Combined BRAF and MEK inhibition in melanoma with BRAF V600 mutations. *The New England Journal of Medicine*, *367*(18), 1694–1703. https://doi.org/10.1056/NEJMoa1210093
25. Glimcher, L. H., Kara, C. J. (1992). Sequences and Factors: A Guide to MHC

Class-II Transcription. *Annual Review of Immunology*, *10*(1), 13–49. https://doi.org/10.1146/annurev.iy.10.040192.000305

26. Grazia, G., Penna, I., Perotti, V., Anichini, A., Tassi, E. (2014). Towards combinatorial targeted therapy in melanoma: from pre-clinical evidence to clinical application (review). *International Journal of Oncology*, *45*(3), 929–949. https://doi.org/10.3892/ijo.2014.2491
27. Greger, J. G., Eastman, S. D., Zhang, V., Bleam, M. R., Hughes, A. M., Smitheman, K. N., Dickerson, S. H., Laquerre, S. G., Liu. L., Gilmer, T. M. (2012). Combinations of BRAF, MEK, and PI3K/mTOR Inhibitors Overcome Acquired Resistance to the BRAF Inhibitor GSK2118436 Dabrafenib, Mediated by NRAS or MEK Mutations. *Molecular Cancer Therapeutics*, *11*(4).
28. Hatzivassiliou, G., Song, K., Yen, I., Brandhuber, B. J., Anderson, D. J., Alvarado, R., Ludlam, M. J. C., Stokoe, D., Gloor, S. L., Vigers, G., Morales, T., Aliagas, I., Liu, B., Sideris, S., Hoeflich, K. P., Jaiswal, B. S., Seshagiri, S., Koeppen, H., Belvin, M., Friedmann, L. S., Malek, S. (2010). RAF inhibitors prime wild-type RAF to activate the MAPK pathway and enhance growth. *Nature*, *464*(7287), 431–435. https://doi.org/10.1038/nature08833
29. Hauschild, A., Grob, J.-J., Demidov, L. V, Jouary, T., Gutzmer, R., Millward, M., Rutkowski, P., Blank, C. U., Miller jr., W. H., Kaempgen, E., Martin-Algarra, S., Karaszewska, B., Mauch, C., Chiarion-Sileni, V., Martin, A.-M., Swann, S., Haney, P., Mirakhur, B., Guckert, M. E., Goodman, V., Chapman, P. B. (2012). Dabrafenib in BRAF-mutated metastatic melanoma: a multicentre, open-label, phase 3 randomised controlled trial. *Lancet (London, England)*, *380*(9839), 358–365. https://doi.org/10.1016/S0140-6736(12)60868-X
30. Hemon, P., Jean-Louis, F., Ramgolam, K., Brignone, C., Viguier, M., Bachelez, H., Triebel, F., Charron, D., Aoudjit, F., Al-Daccak, R., Michel, L. (2011). MHC class II engagement by its ligand LAG-3 (CD223) contributes to melanoma resistance to apoptosis. *Journal of Immunology (Baltimore, Md. : 1950)*, *186*(9), 5173–5183. https://doi.org/10.4049/jimmunol.1002050
31. Homet, B., Ribas, A. (2014). New drug targets in metastatic melanoma. *The Journal of Pathology*, *232*(2), 134–141. https://doi.org/10.1002/path.4259
32. Hunder, N. N., Wallen, H., Cao, J., Hendricks, D. W., Reilly, J. Z., Rodmyre,

R., Jungblut, A., Gnjatic, S., Thompson, J. A., Yee, C. (2008). Treatment of Metastatic Melanoma with Autologous CD4+ T Cells against NY-ESO-1. *New England Journal of Medicine*, *358*(25), 2698–2703. https://doi.org/10.1056/NEJMoa0800251

33. Johnson, D. B., Estrada, M. V., Salgado, R., Sanchez, V., Doxie, D. B., Opalenik, S. R., Vilgelm, A. E., Feld, E., Johnson, A. S., Greenplate, A. R., Sanders, M. E., Lovly, C. M., Frederick, D. T., Kelley, M. C., Richmond, A., Irish, J. M., Shyr, Y., Sullivan, R. J., Puzanov, I., Sosman, J. A., Balko, J. M. (2016). Melanoma-specific MHC-II expression represents a tumour-autonomous phenotype and predicts response to anti-PD-1/PD-L1 therapy. *Nature Communications*, *7*, 10582. https://doi.org/10.1038/ncomms10582
34. Johnson, D. B., Nixon, M. J., Wang, Y., Wang, D. Y., Castellanos, E., Estrada, M. V., Ericsson-Gonzalez, P. I., Cote, C. H., Salgado, R., Sanchez, V., Dean, P. T., Opalenik, S. R., Schreeder, D. M., Rimm, D. L., Kim, J. Y., Bordeaux, J., Loi, S., Horn, L., Sanders, M. E., Ferrel jr., P. B., Xu, Y., Sosman, J. A., Davis, R. S., Balko, J. M. (2018). Tumor-specific MHC-II expression drives a unique pattern of resistance to immunotherapy via LAG-3/FCRL6 engagement. *JCI Insight*, *3*(24). https://doi.org/10.1172/JCI.INSIGHT.120360
35. Kalluri, R., Weinberg, R. A. (2009). The basics of epithelial-mesenchymal transition. *The Journal of Clinical Investigation*, *119*(6), 1420–1428. https://doi.org/10.1172/JCI39104
36. Karin, M., Liu, Z., Zandi, E. (1997). AP-1 function and regulation. *Current Opinion in Cell Biology*, *9*(2), 240–246. https://doi.org/10.1016/S0955-0674(97)80068-3
37. Kirk, G. D., Merlo, C., O' Driscoll, P., Mehta, S. H., Galai, N., Vlahov, D., Samet, J., Engels, E. A. (2007). HIV infection is associated with an increased risk for lung cancer, independent of smoking. *Clinical Infectious Diseases : An Official Publication of the Infectious Diseases Society of America*, *45*(1), 103–110. https://doi.org/10.1086/518606
38. Knutson, K. L., Disis, M. L. (2005). Tumor antigen-specific T helper cells in cancer immunity and immunotherapy. *Cancer Immunology, Immunotherapy*, *54*(8), 721–728. https://doi.org/10.1007/s00262-004-0653-2
39. Krawczyk, M., Reith, W. (2006). Regulation of MHC class II expression, a

unique regulatory system identified by the study of a primary immunodeficiency disease. *Tissue Antigens*, *67*(3), 183–197. https://doi.org/10.1111/j.1399-0039.2006.00557.x

40. Kuzu, O. F., Gowda, R., Sharma, A., Noory, M. A., Kardos, G., Madhunapantula, S. V, Drabick, J. J., Robertson, G. P. (2018). Identification of WEE1 as a target to make AKT inhibition more effective in melanoma. *Cancer Biology & Therapy*, *19*(1), 53–62. https://doi.org/10.1080/15384047.2017.1360446
41. Larkin, J., Chiarion-Sileni, V., Gonzalez, R., Grob, J. J., Cowey, C. L., Lao, C. D., Schadendorf, D., Dummer, R., Smylie, M., Rutkowski, P., Ferrucci, P. F., Hill, A., Wagstaff, J., Carlino, M. S., Haanen, J. B., Maio, M., Marquez-Rodas, I., McArthur, G. A., Ascierto, P. A., Long, G. V., Callahan, M. K., Postow, M. A., Grossmann, K., Sznol, M., Dreno, B., Bastholt, L., Yang, A., Rollin, L. M., Horak, C., Hodi, F. S., Wolchok, J. D. (2015). Combined Nivolumab and Ipilimumab or Monotherapy in Untreated Melanoma. *The New England Journal of Medicine*, *373*(1), 23–34. https://doi.org/10.1056/NEJMoa1504030
42. Lee, N., Zakka, L. R., Schatton, T. (2016). Tumour-infiltrating lymphocytes in melanoma prognosis and cancer immunotherapy. *Pathology*, *48*(2), 177–187. https://doi.org/10.1016/J.PATHOL.2015.12.006
43. Levy, C., Khaled, M., Fisher, D. E. (2006). MITF: master regulator of melanocyte development and melanoma oncogene. *Trends in Molecular Medicine*, *12*(9), 406–414. https://doi.org/10.1016/j.molmed.2006.07.008
44. Linsley, P. S., Brady, W., Grosmaire, L., Aruffo, A., Damle, N. K., Ledbetter, J. A. (1991). Binding of the B cell activation antigen B7 to CD28 costimulates T cell proliferation and interleukin 2 mRNA accumulation. *The Journal of Experimental Medicine*, *173*(3), 721–730.
45. Livak, K., Schmittgen, T. (2001). Analysis of Relative Gene Expression Data Using Real-Time Quantitative PCR and the 2(-Delta Delta C(T)) Method. *Methods (San Diego, Calif.)*, *25*(4). https://doi.org/10.1006/METH.2001.1262
46. Lu, Y.-C., Parker, L. L., Lu, T., Zheng, Z., Toomey, M. A., White, D. E., Yao, X., Li, Y. F., Robbins, P. F., Feldmann, S. A., van der Bruggen, P., Klebanoff, C. A., Goff, S. L., Sherry, R. M., Kammula, U. S., Yang, J. C., Rosenberg, S. A. (2017). Treatment of Patients With Metastatic Cancer Using a Major

Histocompatibility Complex Class II-Restricted T-Cell Receptor Targeting the Cancer Germline Antigen MAGE-A3. *Journal of Clinical Oncology : Official Journal of the American Society of Clinical Oncology*, *35*(29), 3322–3329. https://doi.org/10.1200/JCO.2017.74.5463

47. Madhunapantula, S. V, Robertson, G. P. (2011). Therapeutic Implications of Targeting AKT Signaling in Melanoma. *Enzyme Research*, *2011*, 327923. https://doi.org/10.4061/2011/327923
48. Martins, I., Deshayes, F., Baton, F., Forget, A., Ciechomska, I., Sylla, K., Aoudjit, F., Charron, D., Al-Daccak, R., Alcaide-Loridan, C. (n.d.). Pathologic expression of MHC class II is driven by mitogen-activated protein kinases. https://doi.org/10.1002/eji.200636620
49. Matsushita, K., Takenouchi, T., Shimada, H., Tomonaga, T., Hayashi, H., Shioya, A., Komatsu, A., Matsubara, H., Ochiai, T. (2006). Strong HLA-DR antigen expression on cancer cells relates to better prognosis of colorectal cancer patients: Possible involvement of c-myc suppression by interferon-gammain situ. *Cancer Science*, *97*(1), 57–63. https://doi.org/10.1111/j.1349-7006.2006.00137.x
50. Mendoza, M. C., Er, E. E., Blenis, J. (2011). The Ras-ERK and PI3K-mTOR pathways: cross-talk and compensation. *Trends in Biochemical Sciences*, *36*(6), 320–328. https://doi.org/10.1016/j.tibs.2011.03.006
51. Milella, M., Falcone, I., Conciatori, F., Matteoni, S., Sacconi, A., De Luca, T., Bazzichetto, C., Corbo, V., Simbolo, M., Sperdutti, I., Benfante, A., Del Curatolo, A., Incani, U. C., Malusa, F., Eramo, A., Sette, G., Scarpa, A., Konopleva, M., Andreeff, M., McCubrey, J. A., Blandino, G., Todaro, M., Stassi, G., De Maria, R., Cognetti, F., Del Bufalo, D., Ciuffreda, L. (2017). PTEN status is a crucial determinant of the functional outcome of combined MEK and mTOR inhibition in cancer. *Scientific Reports*, *7*(1), 43013. https://doi.org/10.1038/srep43013
52. Ming, M., He, Y.-Y. (2009). PTEN: New Insights into Its Regulation and Function in Skin Cancer. *The Journal of Investigative Dermatology*, *129*(9), 2109. https://doi.org/10.1038/JID.2009.79
53. Mittal, D., Gubin, M. M., Schreiber, R. D., Smyth, M. J. (2014). New insights into cancer immunoediting and its three component phases—elimination, equilibrium and escape. *Current Opinion in Immunology*, *27*, 16–25.

https://doi.org/10.1016/j.coi.2014.01.004

54. Moloney, F. J., Comber, H., O'Lorcain, P., O'Kelly, P., Conlon, P. J., Murphy, G. M. (2006). A population-based study of skin cancer incidence and prevalence in renal transplant recipients. *The British Journal of Dermatology*, *154*(3), 498–504. https://doi.org/10.1111/j.1365-2133.2005.07021.x
55. Neefjes, J., Jongsma, M. L. M., Paul, P., Bakke, O. (2011). Towards a systems understanding of MHC class I and MHC class II antigen presentation. *Nature Reviews Immunology*, *11*(12), 823. https://doi.org/10.1038/nri3084
56. O'Garra, A., Arai, N. (2000). The molecular basis of T helper 1 and T helper 2 cell differentiation. *Trends in Cell Biology*, *10*(12), 542–550. https://doi.org/10.1016/S0962-8924(00)01856-0
57. Oliveira Cobucci, R. N., Saconato, H., Lima, P. H., Rodrigues, H. M., Prudêncio, T. L., Junior, J. E., Giraldo, P. C., Gonçalves, A. K. da S. (2012). Comparative incidence of cancer in HIV-AIDS patients and transplant recipients. *Cancer Epidemiology*, *36*(2), e69-73. https://doi.org/10.1016/j.canep.2011.12.002
58. Osborn, J. L., Greer, S. F. (2015). Metastatic melanoma cells evade immune detection by silencing STAT1. *International Journal of Molecular Sciences*, *16*(2), 4343–4361. https://doi.org/10.3390/ijms16024343
59. Perera, E., Gnaneswaran, N., Jennens, R., Sinclair, R. (2013). Malignant Melanoma. *Healthcare (Basel, Switzerland)*, *2*(1), 1–19. https://doi.org/10.3390/healthcare2010001
60. Pieper, N., Zaremba, A., Leonardelli, S., Harbers, F. N., Schwamborn, M., Lübcke, S., Schroers, B., Baingo, J., Schramm, A., Haferkamp, S., Seifert, U., Sucker, A., Lennerz, V., Wölfel, T., Schadendorf, D., Schilling, B., Paschen, A., Zhao, F. (2018). Evolution of melanoma cross-resistance to CD8 $^{+}$ T cells and MAPK inhibition in the course of BRAFi treatment. *OncoImmunology*,e1450127. https://doi.org/10.1080/2162402X.2018.1450127
61. Psaty, E. L., Scope, A., Halpern, A. C., Marghoob, A. A. (2010). Defining the patient at high risk for melanoma. *International Journal of Dermatology*, *49*(4), 362–376. https://doi.org/10.1111/j.1365-4632.2010.04381.x
62. Redman, J. M., Gibney, G. T., Atkins, M. B. (2016). Advances in

immunotherapy for melanoma. *BMC Medicine*, *14*, 20. https://doi.org/10.1186/s12916-016-0571-0

63. Robert, C., Karaszewska, B., Schachter, J., Rutkowski, P., Mackiewicz, A., Stroiakovski, D., Lichinitiser, M., Dummer, R., Grange, F., Mortier, L., Chiarion-Saleni, V., Drucis, K., Krajsova, I., Hauschild, A., Lorigan, P., Wolter, P., Long, G. V., Flaherty, K., Nathan, P., Ribas, A., Martin, A.M., Sun, P., Crist, W., Legos, J., Rubin, S.D., Little, S.M., Schadendorf, D. (2015). Improved overall survival in melanoma with combined dabrafenib and trametinib. *The New England Journal of Medicine*, *372*(1), 30–39. https://doi.org/10.1056/NEJMoa1412690
64. Rodig, S. J., Gusenleitner, D., Jackson, D. G., Gjini, E., Giobbie-Hurder, A., Jin, C., Chang, H., Lovitch, S.B., Horak, C., Weber, J.S., Weirather, J.L., Wolchok, J.D., Postow, M.A., Pavlick, A.C., Chesney, J., Hodi, F. S. (2018). MHC proteins confer differential sensitivity to CTLA-4 and PD-1 blockade in untreated metastatic melanoma. *Science Translational Medicine*, *10*(450), eaar3342. https://doi.org/10.1126/scitranslmed.aar3342
65. Rodríguez, T., Méndez, R., Del Campo, A., Aptsiauri, N., Martín, J., Orozco, G., Pawelec, G., Schadendorf, D., Ruiz-Cabello, F., Garrido, F. (2007). Patterns of constitutive and IFN-gamma inducible expression of HLA class II molecules in human melanoma cell lines. *Immunogenetics*, *59*(2), 123–133. https://doi.org/10.1007/s00251-006-0171-9
66. Schadendorf, M. D., Van Akkooi, A. C. J., Berking, C., Griewank, K. G., Gutzmer, R., Hauschild, A., Stang, A., Roesch, A., Ugurel, S. (2018). *Melanoma*. *The Lancet* (Vol. 392). https://doi.org/10.1016/S0140-6736(18)31559-9
67. Scharer, C. D., Choi, N. M., Barwick, B. G., Majumder, P., Lohsen, S., Boss, J. M. (2015). Genome-wide CIITA-binding profile identifies sequence preferences that dictate function versus recruitment. *Nucleic Acids Research*, *43*(6), 3128–3142. https://doi.org/10.1093/nar/gkv182
68. Serrano, M. (1997). The tumor suppressor protein p16INK4a. *Experimental Cell Research*, *237*(1), 7–13. https://doi.org/10.1006/excr.1997.3824
69. Shain, A. H., Bastian, B. C. (2016). From melanocytes to melanomas. *Nat Rev Cancer*, *16*(6), 345–358.
70. Shurin, M. R. (2012). Cancer as an immune-mediated disease.

ImmunoTargets and Therapy, *1*, 1–6. https://doi.org/10.2147/ITT.S29834

71. Sosman, J. A., Kim, K. B., Schuchter, L., Gonzalez, R., Pavlick, A. C., Weber, J. S., McArthur, G. A., Hutson, T. E., Moschos, S. J., Flaherty, K. T., Hersey, P., Kefford, R., Lawrence, D., Puzanov, I., Lewis, K. D., Amaravadi, R. K., Chmielowski, B., Lawrence, H. J., Shyr, Y., Ye, F., Li, J., Nolop, K. B., Lee, R. J., Joe, A. K., Ribas, A. (2012). Survival in BRAF V600-mutant advanced melanoma treated with vemurafenib. *The New England Journal of Medicine*, *366*(8), 707–714. https://doi.org/10.1056/NEJMoa1112302
72. Stahl, J. M., Cheung, M., Sharma, A., Trivedi, N. R., Shanmugam, S., Robertson, G. P. (2003). Loss of PTEN Promotes Tumor Development in Malignant Melanoma. *Cancer Research*, *63*(11).
73. Steimle, V., Siegrist, C. A., Mottet, A., Lisowska-Grospierre, B., Mach, B. (1994). Regulation of MHC class II expression by interferon-gamma mediated by the transactivator gene CIITA. *Science (New York, N.Y.)*, *265*(5168), 106–109.
74. Su, H., Na, N., Zhang, X., Zhao, Y. (2017). The biological function and significance of CD74 in immune diseases. *Inflammation Research*, *66*(3), 209–216. https://doi.org/10.1007/s00011-016-0995-1
75. Tanaka, R., Koyanagi, K., Narita, N., Kuo, C., Hoon, D. S. B. (2011). Prognostic molecular biomarkers for cutaneous malignant melanoma. *Journal of Surgical Oncology*, *104*(4), 438–446. https://doi.org/10.1002/jso.21969
76. Tay, R. E., Richardson, E. K., Toh, H. C. (2020). Revisiting the role of CD4+ T cells in cancer immunotherapy—new insights into old paradigms. *Cancer Gene Therapy*, 1–13. https://doi.org/10.1038/s41417-020-0183-x
77. ten Broeke, T., Wubbolts, R., Stoorvogel, W. (2013). MHC class II antigen presentation by dendritic cells regulated through endosomal sorting. *Cold Spring Harbor Perspectives in Biology*, *5*(12), a016873. https://doi.org/10.1101/cshperspect.a016873
78. Tietze, J. K., Forschner, A., Loquai, C., Mitzel-Rink, H., Zimmer, L., Meiss, F., Rafei-Shamsabadi, D., Utikal, J., Bergmann, M., Meier, F., Kreuzberg, N., Schlaak, M., Weishaupt, C., Pföhler, C., Ziemer, M., Fluck, M., Rainer, J., Heppt, M. V., Berking, C. (2018). The efficacy of re-challenge with BRAF inhibitors after previous progression to BRAF inhibitors in melanoma: A

retrospective multicenter study. *Oncotarget*, *9*(76), 34336–34346. https://doi.org/10.18632/oncotarget.26149

79. Tolcher, A. W., Bendell, J. C., Papadopoulos, K. P., Burris, H. A., Patnaik, A., Jones, S. F., Rasco, D., Cox, D.S., Durante, M., Bellew, K.M., Park, J., Le, N.T., Infante, J. R. (2015). A phase IB trial of the oral MEK inhibitor trametinib (GSK1120212) in combination with everolimus in patients with advanced solid tumors. *Annals of Oncology*, *26*(1), 58–64. https://doi.org/10.1093/annonc/mdu482
80. Tuthill, R. J., Unger, J. M., Liu, P. Y., Flaherty, L. E., Sondak, V. K., & Southwest Oncology Group. (2002). Risk assessment in localized primary cutaneous melanoma: a Southwest Oncology Group study evaluating nine factors and a test of the Clark logistic regression prediction model. *American Journal of Clinical Pathology*, *118*(4), 504–511. https://doi.org/10.1309/WBF7-N8KH-71KT-RVQ9
81. Vesely, M. D., Schreiber, R. D. (2013). Cancer immunoediting: antigens, mechanisms, and implications to cancer immunotherapy. *Annals of the New York Academy of Sciences*, *1284*(1), 1–5. https://doi.org/10.1111/nyas.12105
82. Webb, E. S., Liu, P., Baleeiro, R., Lemoine, N. R., Yuan, M., Wang, Y.-H. (2018). Immune checkpoint inhibitors in cancer therapy. *Journal of Biomedical Research*, *32*(5), 317–326. https://doi.org/10.7555/JBR.31.20160168
83. Wellbrock, C., Weisser, C., Hassel, J. C., Fischer, P., Becker, J., Vetter, C. S., Behrmann, I., Kortylewski, M., Heinrich, P.C., Schartl, M. (2005). STAT5 Contributes to Interferon Resistance of Melanoma Cells. *Current Biology*, *15*(18), 1629–1639. https://doi.org/10.1016/j.cub.2005.08.036
84. Werzowa, J., Koehrer, S., Strommer, S., Cejka, D., Fuereder, T., Zebedin, E., Wacheck, V. (2011). Vertical inhibition of the mTORC1/mTORC2/PI3K pathway shows synergistic effects against melanoma in vitro and in vivo. *The Journal of Investigative Dermatology*, *131*(2), 495–503. https://doi.org/10.1038/jid.2010.327
85. Wu, H., Goel, V., Haluska, F. G. (2003). PTEN signaling pathways in melanoma. *Oncogene*, *22*(20), 3113–3122. https://doi.org/10.1038/sj.onc.1206451

86. Zhang, H., Dutta, P., Liu, J., Sabri, N., Song, Y., Li, W. X., Li, J. (2019). Tumour cell-intrinsic CTLA4 regulates PD-L1 expression in non-small cell lung cancer. *Journal of Cellular and Molecular Medicine*, *23*(1), 535–542. https://doi.org/10.1111/jcmm.13956

8 LIST OF FIGURES

9 LIST OF TABLES

10 ABBREVIATIONS

AG	Arbeitsgruppe, research group
AB	Antibody
ACT	Adoptive Cell-Transfer
AKT	Protein Kinase B
AP-1	Activating Protein 1
APC	Antigen presenting cell
APS	Ammonium persulfate
BSA	Bovine serum albumin
CIITA	MHC Class-II Trans-Activator
cAMP	Cyclic adenosine monophosphate
CD	Cluster of Differentiation
CD74	Cluster of Differentiation 74
CDK	Cyclin dependent kinase
cDNA	complementary DNA
CO_2	Carbon dioxide
CTL	Cytotoxic lymphocyte
DC	Dendritic cell
DMSO	Dimethylsulfoxid
DNA	Deoxyribonucleic acid
dNTP	deoxynucleotide triphosphate
ECL	enhanced chemiluminescence
EDTA	Ethylenediaminetetraacetic acid
ERK	extracellular signal related kinase
EtOH	Ethanol
FACS	Fluorescence-activated cell scanning
FBS	Fetal Bovine Serum
Fig.	Figure
g	G-Force
GAPDH	Glyceraldehyde-3-phosphate-dehydrogenase
gDNA	genomic DNA
h	hour(s)

H_2O_2	Hydrogen peroxide
HLA	Human Leukocyte Antigen
JNK	c-Jun N-Terminal kinase
mAb	mouse Antibody
MAPK	Mitogen-activated protein kinase
Melan-A (MART1)	Melanoma antigen recognized by T cells 1
MeOH	Methanol
min	Minute
MITF	Microphtalmia Transcription factor
ml	Milliliter
mM	Millimolar
mRNA	messenger-RNA
n	Sample size
nm	Nanometer
nM	Nanomolar
PBS	Phosphat buffered saline
PCR	Polymerase chain reaction
PI3K	Phosphoinositide 3-kinase
PIP3	Phosphatidylinositol (3,4,5)-trisphosphate
PMSF	Phenylmethanesulfonyl Fluoride
P/S	Penicillin/Streptomycin
qPCR	quantitative reverse transcriptase PCR
RNA	Ribonucleic acid
RT	Room temperature
Rpm	Rounds per Minute
RPMI	Roswell Park Memorial Institute
sec	Seconds
SEM	Standard error of mean
SDS	Sodium Dodecyl Sulphate
Tab.	Table
TEMED	N, N, N´, N´-Tetramethylethylenediamine
TIL	Tumor infiltrating lymphocyte
T-reg.	Regulatory T-cell
Tris	Tris (hydroxymethyl) aminomethane

µg	Microgram
µm	Micrometer

11 SUPPLEMENTARY FIGURES

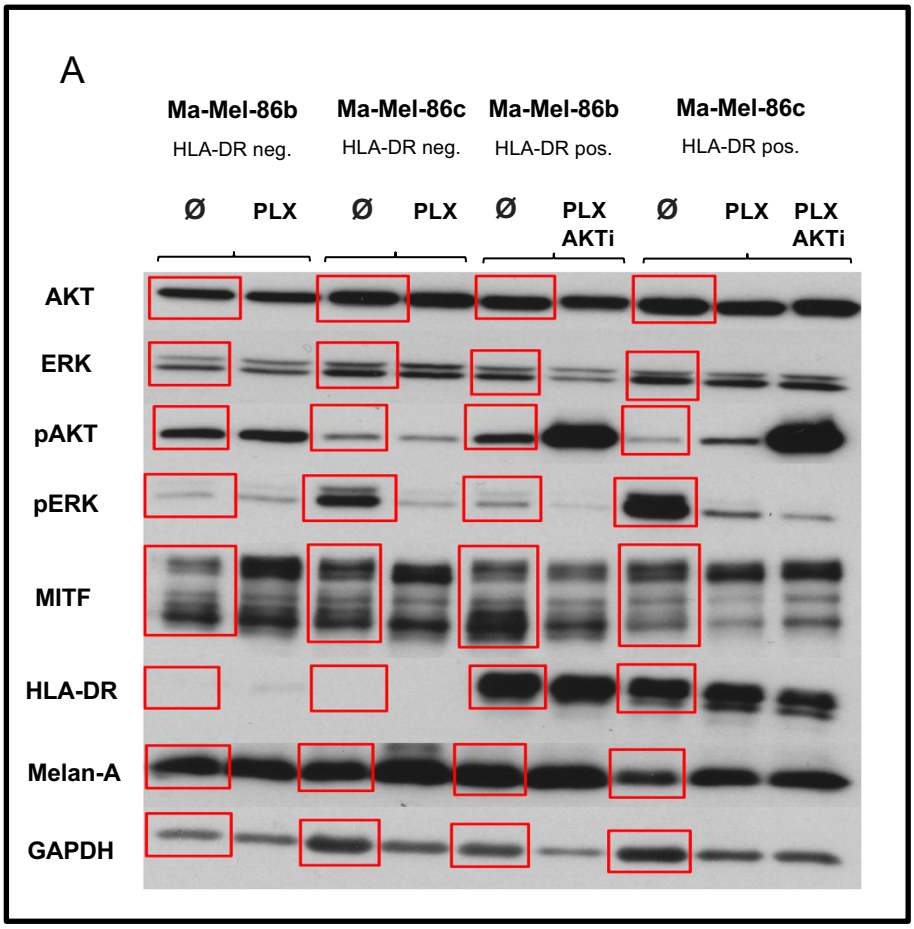

Supplementary Figure 1 A
Full blots of immunoblots shown in the main figure (Fig. 1.4) of the manuscript. The respective main figures are indicated.
DMSO (control Ø), 1 µM BRAFi (PLX) and 1 µM PLX + 2 µM Akt-Inhibitor (PLX+AKTi).

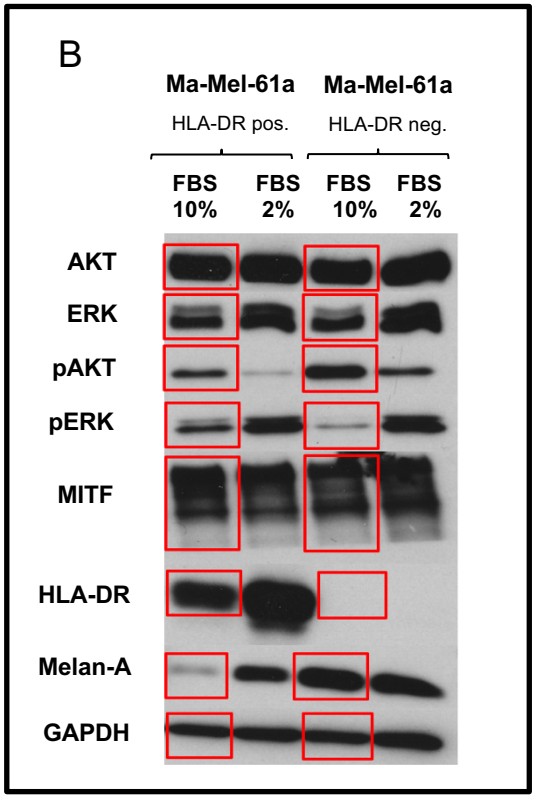

Supplementary Figure 1 B
Full blots of immunoblots shown in the main figure (Fig. 1.4) of the manuscript. The respective main figures are indicated.
FBS 10% is the cell culture supplement used throughout all experiments, FBS 2% medium used to starve cells before invasion essay.

12 CURRICULUM VITAE

Der Lebenslauf ist in der Online-Version aus Gründen des Datenschutzes nicht enthalten.

Der Lebenslauf ist in der Online-Version aus Gründen des Datenschutzes nicht enthalten.

Der Lebenslauf ist in der Online-Version aus Gründen des Datenschutzes nicht enthalten.